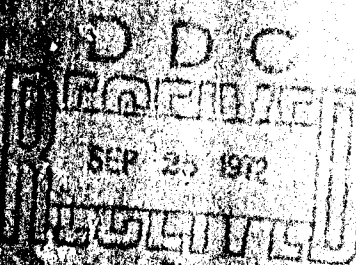


748656

4 PLATE 1 BE

High Strain Engineering Mechanics  
PENNSYLVANIA STATE UNIVERSITY



Office of Naval Research  
No. N00014-67-A-0386-Subn.  
Progress Report No. 3

**Best Available Copy**

Unclassified  
Security Classification

**DOCUMENT CONTROL DATA - R&D**

(Security classification of title, body of abstract and indexing annotation must be entered when the overall report is classified)

1. ORIGINATING ACTIVITY (Corporate author)  The Pennsylvania State University	2a. REPORT SECURITY CLASSIFICATION  Unclassified
	2b. GROUP  N.A.

3. REPORT TITLE

Dynamic Response of Viscoplastic Beams

4. DESCRIPTIVE NOTES (Type of report and inclusive dates)

Progress Report No. 3 (October 1971 through August 1972)

5. AUTHOR(S) (Last name, first name, initial)

Neubert, V. H., DiMarcello, R., Vogel, W., and Weiss, R.

6. REPORT DATE  August 1972	7a. TOTAL NO. OF PAGES  49	7b. NO. OF REFS  6
8a. CONTRACT OR GRANT NO.  N00014-67- <del>1</del> 385-0010	9a. ORIGINATOR'S REPORT NUMBER(S)  Progress Report No. 3	
b. PROJECT NO.		
c.	9b. OTHER REPORT NO(S) (Any other numbers that may be assigned this report)	
d.		

10. AVAILABILITY/LIMITATION NOTICES

Qualified requestors may obtain copies of this report from DDC.

11. SUPPLEMENTARY NOTES  None	12. SPONSORING MILITARY ACTIVITY  Office of Naval Research Naval Research Laboratory Washington, D. C.
-------------------------------------	--

13. ABSTRACT

There are three parts to the report. The first part presents results of shock tests on rectangular steel beams. The constants in a moment-curvature relationship, which includes rate effects, are related to experimental data. The second part presents a relationship between material parameters obtained from tension-compression tests to those in the moment-curvature equation. The third part presents theoretical response of a viscoplastic cantilever beam to a shock input.

14. Key Words

Shock, Viscoplastic, Beams, Bending, Elastoplastic, Material Behavior, Steel

Dynamic Response of Viscoplastic Beams

by

Vernon H. Neubert

Department of Engineering Mechanics  
The Pennsylvania State University

Reproduction in whole or in part  
is permitted for any purpose of  
the United States Government

Office of Naval Research  
Contract No. N00014-67-A-0385-0010  
Progress Report No. 3

August 1972

## AUTHORIZATION

This work was performed under ONR Contract No. N00014-67-A-0385-0010-03, under the technical supervision of Naval Research Laboratory, and under the sponsorship and funding of Defense Nuclear Agency under its Nuclear Weapons Effects Program, Subtask NB002-04.

## BACKGROUND

This is the third progress report prepared under the contract listed above. The two previous progress reports dealt primarily with the derivation of improved finite elements for elastic Bernoulli-Euler and Timoshenko beam segments. The present report deals with experiments and analysis performed to arrive at analysis procedures and failure criteria for structures deformed into the plastic range. This report contains three separate parts:

	<u>Pages</u>
I. Experimental Dynamic Response of a Viscoplastic Beam Segment R. DiMarcello and V. H. Neubert	1-16
II. Relationship Between Moment-Curvature and Stress-Strain Constitutive Relationships W. Vogel and V. H. Neubert	17-21
III. Theoretical Response of an Idealized Viscoplastic Cantilever Beam R. Weiss and V. H. Neubert	22-46

## TABLE OF CONTENTS

	<u>Page</u>
I. Experimental Dynamic Response of a Viscoplastic Beam Segment	1
Background	1
Description of the Apparatus	2
Material	3
Test Results	4
Relationship Between C and the Time Delay	5
Results and Conclusions	8
II. Relationship Between Moment-Curvature and Stress-Strain Constitutive Relationships	17
III. Theoretical Response of an Idealized Viscoplastic Cantilever Beam	22
Introduction	22
Equation of Motion	26
Beams Studied Using a Constant $L_2$	30
Results Using a Variable $L_2$	31
Summary and Conclusions	33
References	47

## LIST OF FIGURES

<u>Figure</u>	<u>Page</u>
1 Elevation and Plan Views of Apparatus	10
2 Instrumentation	11
3 Experimental Static Moment vs. Curvature	12
4 Static and Dynamic Moment vs. Curvature	13
5 Dynamic Moment vs. Curvature - Repeated 10 inch Drops	14
6 Dynamic Moment vs. Curvature - Successive 10, 12 and 14 inch Drops	15
7 Strain Records vs. Time on Oscilloscope	16
8 Cantilever Beam With Viscoelastic Region	21
9 Bi-Linear Static Moment vs. k	24
10 Two-Segment Viscoplastic Beam	24
11 $\ddot{y}_o$ vs. t	25
12 $y_1$ vs. t, Various R, $L_2 = 0.05$ inches	34
13 $y_1$ vs. t, Various R, $L_2 = 0.25$ inches	35
14 $y_1$ vs. t, Various R, $L_2 = 0.50$ inches	36
15 $y_1$ vs. t, Various R, $L_2 = 1.0$ inches	37
16 $y_1$ vs. t, Various R, $L_2 = 5.0$ inches	38
17 $M_2$ vs. t, Various R, $L_2 = 0.05$ inches	39
18 $M_2$ vs. t, Various R, $L_2 = 0.25$ inches	40
19 $M_2$ vs. t, Various R, $L_2 = 0.5$ inches	41
20 $M_2$ vs. t, Various R, $L_2 = 1.0$ inches	42
21 $y_1$ vs. t, R = .1, $L_2$ Variable Compared With $L_2$ Constant	43
22 $y_1$ vs. t, R = 1, $L_2$ Variable Compared With $L_2$ Constant	44

## LIST OF FIGURES (continued)

<u>Figure</u>		<u>Page</u>
23	$L_2$ vs. $t$ , $R = .1$ and $1$	45
24	$M_2$ vs. $t$ , $L_2$ a Variable, $R = .1$ and $1$	46

## I. Experimental Dynamic Response of a Viscoplastic Beam Segment

R. DiMarcello and V. H. Neubert

### Background

The writers and associates have conducted a series of tests of viscoplastic beams under dynamic loading. The relation of this work to that of others in the literature has been summarized in past reports<sup>(1)</sup> and will not be reported here. However, enough of the local work will be reviewed to show the motive for the study reported herein.

Stanovsky<sup>(2)</sup> carried out experiments on cantilever steel beams of rectangular cross-section. The beams carried a tip mass and were loaded by a mechanical impactor which struck the tip mass. A pressure transducer between the mass and the impactor measured the applied force, which was used to predict the measured strain. One of the primary conclusions of Stanovsky's work was that, for mild steel, the experimental strain lagged behind the strain predicted using a bilinear stress-strain relationship. This led to the study of the following moment-curvature relationship

$$EI\dot{\kappa} = \dot{M} + C(M - M_{st}) \quad (1)$$

by Brown<sup>(3)</sup>. Equation (1) is similar in form to a stress-strain suggested by Malvern<sup>(4)</sup> and studied by Plass<sup>(5)</sup> and others. A derivation of Equation (1) starting with the stress-strain relationship

is given in Part II of this report. Brown performed experiments on cantilever beams in a shock machine. Moments were calculated based on measured accelerations of the tip masses. Curvature was deduced from strain measurements. Brown suggested values of C for Equation (1) in the range of  $C = 500$  to  $3000$  for a  $1" \times 1/8"$  beam. Subsequently tests involving three parallel beams carrying a common tip mass were carried out on the shock machine at the Naval Research Laboratory. Again the moments were computed from measured accelerations of the tip mass. Static tests of beams of the same material were made. Vogel<sup>(1,6)</sup> predicted the dynamic response from measured base acceleration and found that Equation (1) a satisfactory moment-curvature relationship using values of C in approximately the same range as proposed by Brown. One unexpected result of these tests at the Naval Research Laboratory was that the measured dynamic moment was less than the measured static moment just after yielding of the outer beam fibers. It was not determined whether this was a property of the material or due to errors in measurements. The main purpose of the present experiments was to study the same beam cross-section, but to use a different experimental method for deducing the applied moment.

#### Description of the Apparatus

The apparatus is shown in Figure 1. The beam was 1 inch wide,  $1/4$  inch deep, and 18 inches long. It carried a steel tip mass bolted on at each end. There were two supports which were designed to act approximately as simple hinge-type supports. The experimental segment was a machined-down region at the center-line  $1/8$  inch thick, 1 inch wide, and 1 inch long. The apparatus had two features that were

significantly different from those of previous tests: (1) the test segment was in a region to which the shear should have been a minimum and (2) the moment was deduced from strain gauges at locations 1 and 4 where the beam material remained essentially elastic.

The beam supports were bolted to a base which was in turn bolted to the table of the IMPAC shock machine, the same shock machine used by Brown. The acceleration pulse provided at the shock machine table is approximately a half-sine wave with a 20 millisecond duration.

Strains were measured using Micromeasurement foil gauges 1/8 inch long. Ellis BAM-1 bridge amplifiers were used with one arm active and the signals were photographed on a Tektronix oscilloscope (Figure 2).

Static tests were performed using the same beam and support arrangement on the table of a Tinius-Olsen machine. The tip masses were removed and the load applied to the two ends simultaneously by an attachment to the moving head of the machine. Moments were deduced from strain measurements at gauges 1 and 4 and curvature from gauges 2 and 3, as in the dynamic tests. Moments were also calculated from the total load applied by the machine. These were not in close agreement with the moments measured at stations 1 and 4. The difference was assumed to be due to moment restraint provided by the "hinged" supports.

#### Material

The material was a 1020 steel, cold-rolled and annealed, after machining, at 800°C for one hour.

Test Results

Measurements from gauges 1 and 4 showed that the arrangement and response were symmetrical. It was assumed that the moment was not a function of position between the supports. In Figure 3 the moment versus curvature from two static tests is plotted as obtained at gauges 2 and 3. In Figure 4 a static curve is compared with a dynamic curve obtained from a 10 inch drop of the shock machine. The data tends to confirm that obtained on the Naval Research Laboratory shock machine in that the elastic stiffness EI is about the same under dynamic and static loading. Also, shortly after the outer fibers yield, at about 120 inch-pounds, the dynamic moment becomes less than the static moment for the same curvature. As the loading increases, the dynamic moment again exceeds the static moment. Thus, the "sag" in the dynamic moment curvature curve again is evident.

In Figure 5 the same dynamic curve shown in Figure 4 is shown as curve 1 and compared with that from another specimen. The curve numbered 1 represented the first test of a beam. The curves 2, 3, 4 and 5 were successive 10 inch drops of another beam that had previously been dropped several times. The curves show the effect of reloading. The behavior is not completely understood, but this trend on successive drops toward greater curvature for the same moment is obvious.

In Figure 6, the result of increasing the drop height on successive tests is shown. Curve 1 is the result of a 10 inch drop following the drop which produced curve 5 of Figure 5. Curves 2 and 3 resulted from successive 12 and 14 inch drops. Note that the curvature scale on Figure 6 is different from that of Figures 3, 4 and 5.

One of the points of primary interest in the present data is the time delay between the occurrence of maximum moment and maximum curvature. This time delay can be directly related to the constant C in Equation (1). The following simple mathematical exercise will help show this relationship.

#### Relationship Between C and the Time Delay

The purpose here is to assume a simple form of moment loading and solve Equation (1) for the resulting curvature in order to relate the constants to associated phase angle or time delay between maximum moment and maximum curvature.

During the elastic range it is immaterial as to the time and rate of loading. In the plastic range the loading is assumed to be sinusoidal. The following theoretical moment-time input is used:

$$M = S_1 k = S_1 c_o t \quad 0 \leq t \leq t_o \quad (2)$$

$$M = S_1 k_y = M_y \quad t = t_o \quad (3)$$

$$M = S_1 k_y + \frac{S_1 c_o}{\omega} \sin \omega(t-t_o) \quad t \geq t_o \quad (4)$$

Here  $k_y$  is the curvature at the knee of a typical moment-curvature plot, and is attained when nearly the entire cross-section begins to undergo plastic deformation. Also  $S_1 = EI$  is the elastic bending stiffness. In terms of symbols used in reference (1), Equation (1) could be written

$$\dot{k} = \frac{\dot{M}}{S_1} + R(M - M_{st}) \quad (5)$$

Here  $R S_1 = C.$

During elastic loading  $M = M_{st}$ , so

$$k = c_0 t \quad 0 \leq t \leq t_0 \quad (6)$$

$$\text{and} \quad k = k_y \quad t = t_0 \quad (7)$$

For  $t \geq t_0$ , we assume a bi-linear static moment curvature relationship:

$$M_{st} = M_y + S_2 (k - k_y) \quad (8)$$

Substituting (8) into (5) yields the following linear differential equation:

$$\dot{k} + RS_2 k = \frac{\dot{M}}{S_1} + RM + R[S_2 k_y - M_y] \quad \text{for } t \geq t_0 \quad (9)$$

With  $M$  as prescribed in (5), the resulting solution for  $k$  is

$$k = k_y + d_1 e^{\frac{-(t-t_0)}{RS_2}} - d_1 \cos \omega(t-t_0) + d_2 \sin \omega(t-t_0) \quad (10)$$

where  $d_1 = \frac{R \alpha \omega (S_1 - S_2)}{S_1 (\omega^2 - RS_2)}$

$$d_2 = \frac{(a\omega^2 + R^2 a S_1 S_2)}{S_1(\omega^2 - RS_2)}$$

and  $a = \frac{S_1 c_o}{\omega}$

Considering only the sine and cosine terms in (10) the phase angle  $\phi$  between moment as prescribed in (4) and curvature  $k$  is

$$\tan \phi = \frac{d_1}{d_2}$$

$$\tan \phi = \frac{R \omega (S_2 - S_1)}{\omega^2 + R^2 S_1 S_2} \quad (11)$$

For the present data, it appears that  $\omega^2 \ll R^2 S_1 S_2$ .

$$\text{Then } \tan \phi \approx \frac{\omega (S_2 - S_1)}{RS_1 S_2} \quad (12)$$

If, in addition,  $S_2 \ll S_1$

$$\tan \phi \approx - \frac{\omega}{RS_2} \quad (13)$$

Letting  $\phi = \omega\tau$ , with  $\tau$  the time delay,  
and  $\tan \phi \approx \phi$ , then from (12)

$$\tau \approx \frac{S_2 - S_1}{RS_1 S_2} \quad (14)$$

Since  $C = RS_1$ , from (14)

$$C \approx \frac{S_2 - S_1}{\tau S_2} \quad (15)$$

The value of  $\tau$  can be scaled directly from data, such as that of Figure 7. If  $\tau = -0.2 \times 10^{-2}$  sec. and  $S_2 = 0.2 S_1$ ,

$$C \approx 2000.$$

$$\text{With } S_1 = 5000, R \approx 0.4.$$

Note that  $RS_2 \approx 1600$  and the exponential term in Equation (10) drops out quickly.

#### Results and Conclusions

The purpose of the work was to test the same rectangular beam cross-section using a different apparatus for direct measurement of the moment-curvature relationship on first loading:

(1) The result of previous tests with accelerometers appears to be confirmed; namely, that the dynamic moment becomes less than the static moment shortly after yielding of the outer beam fibers occurs. This is apparently in conflict with Equation (1) and the common assumption that plastic flow will not occur unless the dynamic stress is greater than the static stress.

(2) An equation is presented for estimating the value of  $C$  in Equation (1) directly from the measured time delay. The value obtained for the present data for commercially annealed steel is in the range of that proposed by Brown<sup>(3)</sup> and Vogel<sup>(6)</sup> based on more thorough analyses.

(3) The apparatus has several advantages over a cantilever beam arrangement. One is that there is practically no shear in the specimen. A second is that some of the difficulties of deducing load from acceleration measurements are eliminated. A third is that the distance between the point where moment is sensed and curvature measured is greatly reduced. Also most of the material between the two points remains elastic, so there is little likelihood of the time delay being due to wave travel time between the two points.

(4) The study has dealt primarily with first loading of the specimen. However, the data from reloading of the same specimen, especially Figure 5, bears further study. Brown gave examples of similar behavior. The fact that the moment is always less on reloading than on the previous loading was initially unexpected. There had been speculation that Equation (1) could be used for the  $i^{\text{th}}$  reloading if  $M_{st}$  were replaced by  $M_{i-1}$ , the relationship obtained from the previous dynamic loading. The present data indicates that prediction of response to reloading requires considerably more study.

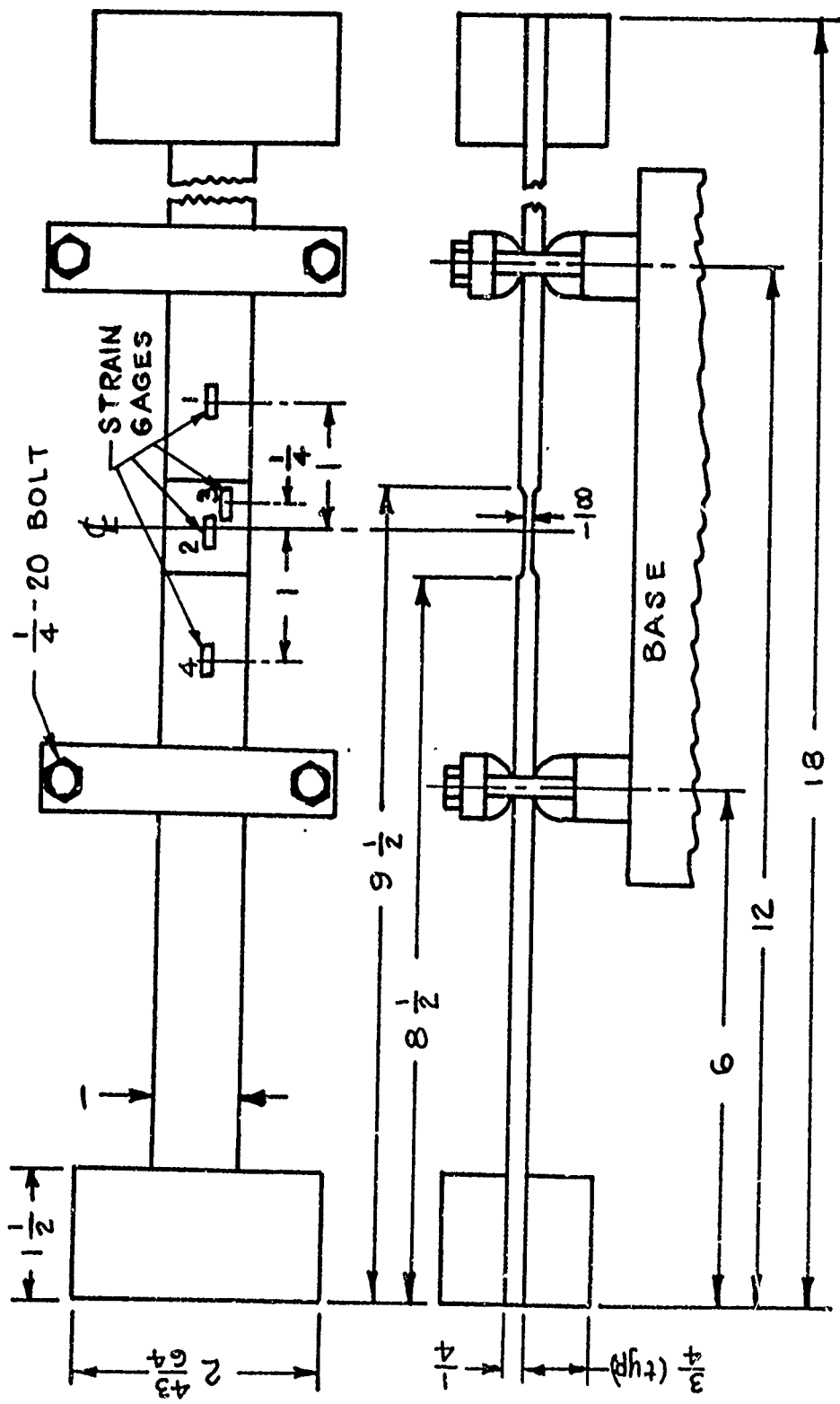


Fig. 1 Elevation and Plan Views of Apparatus

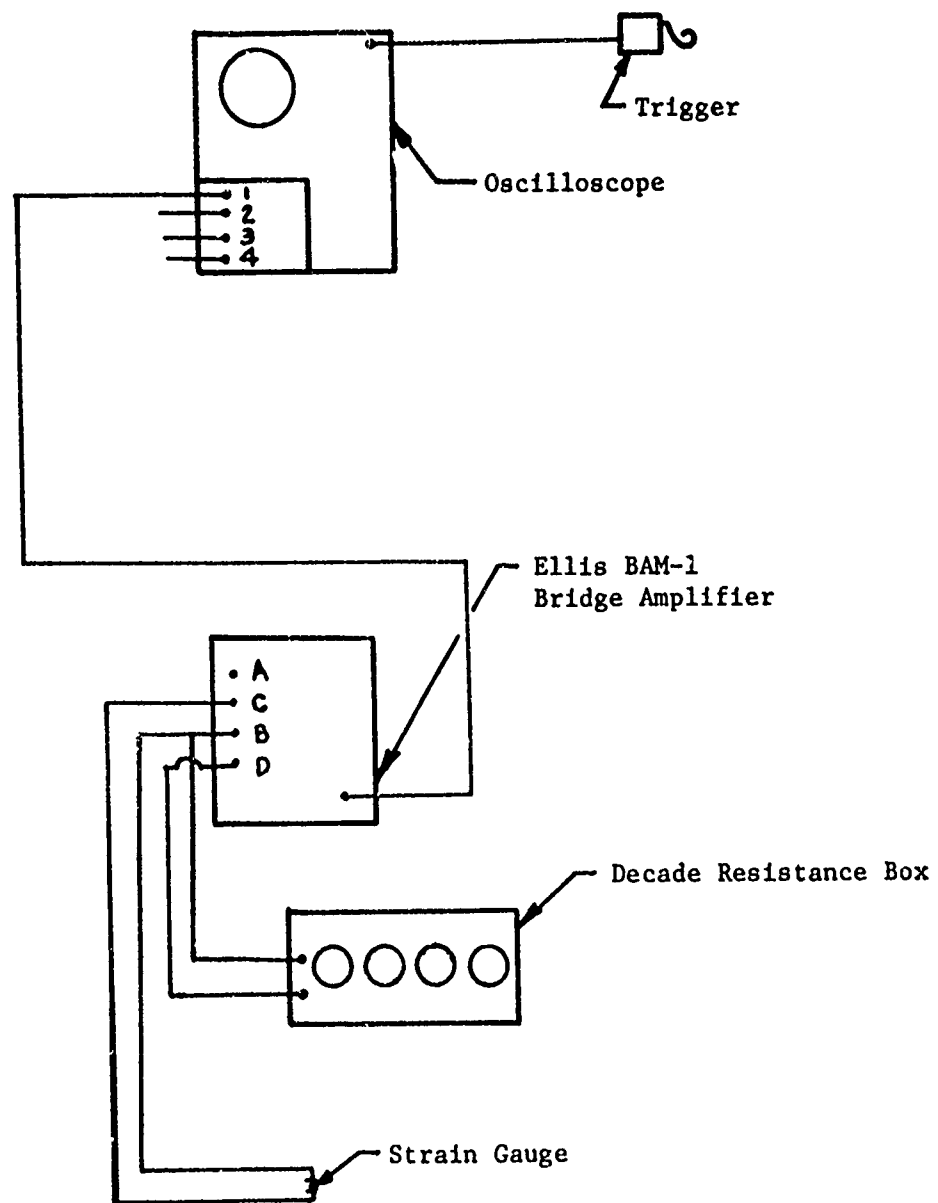


Fig. 2 Instrumentation

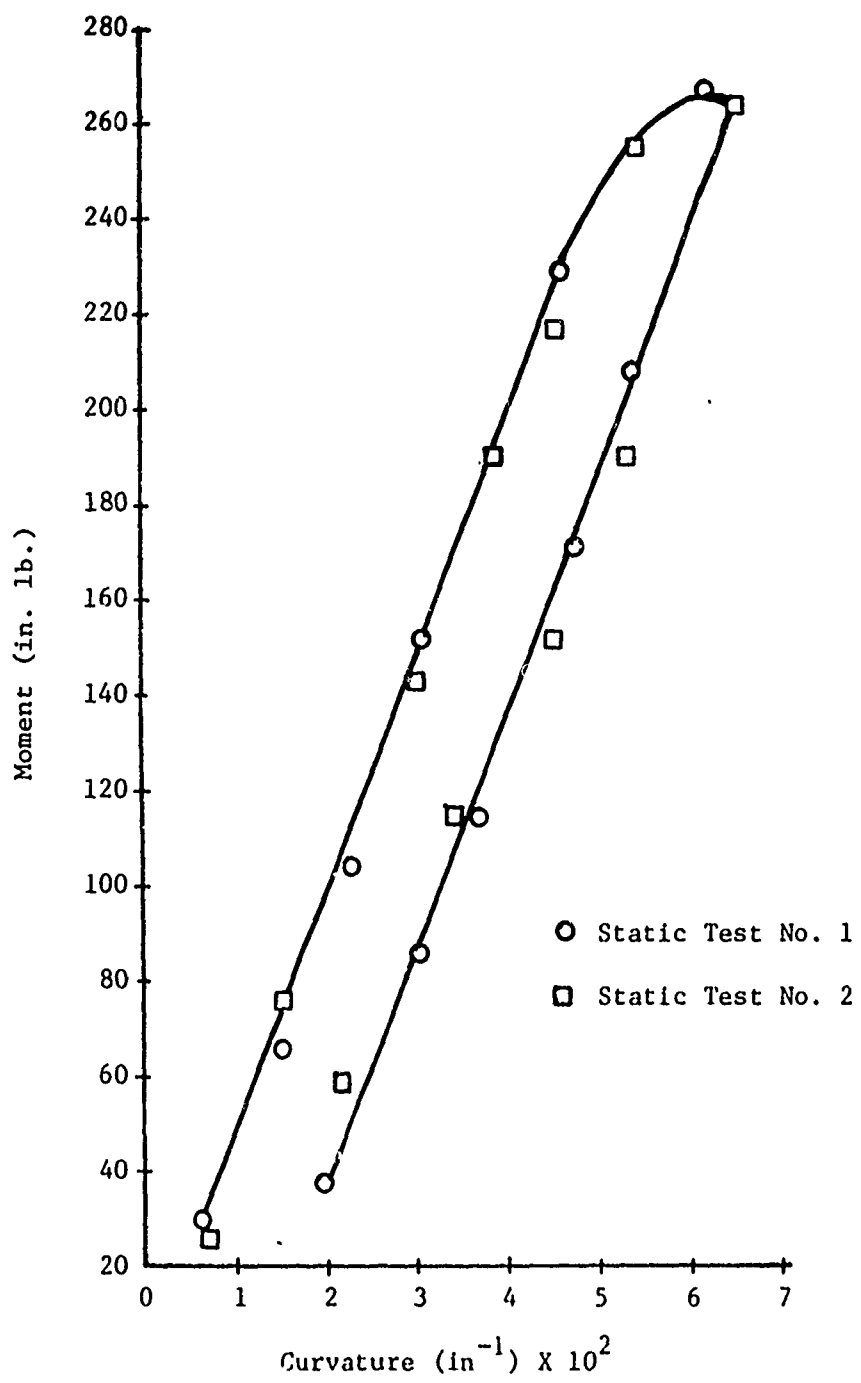


Fig. 3 Experimental Static Moment vs. Curvature

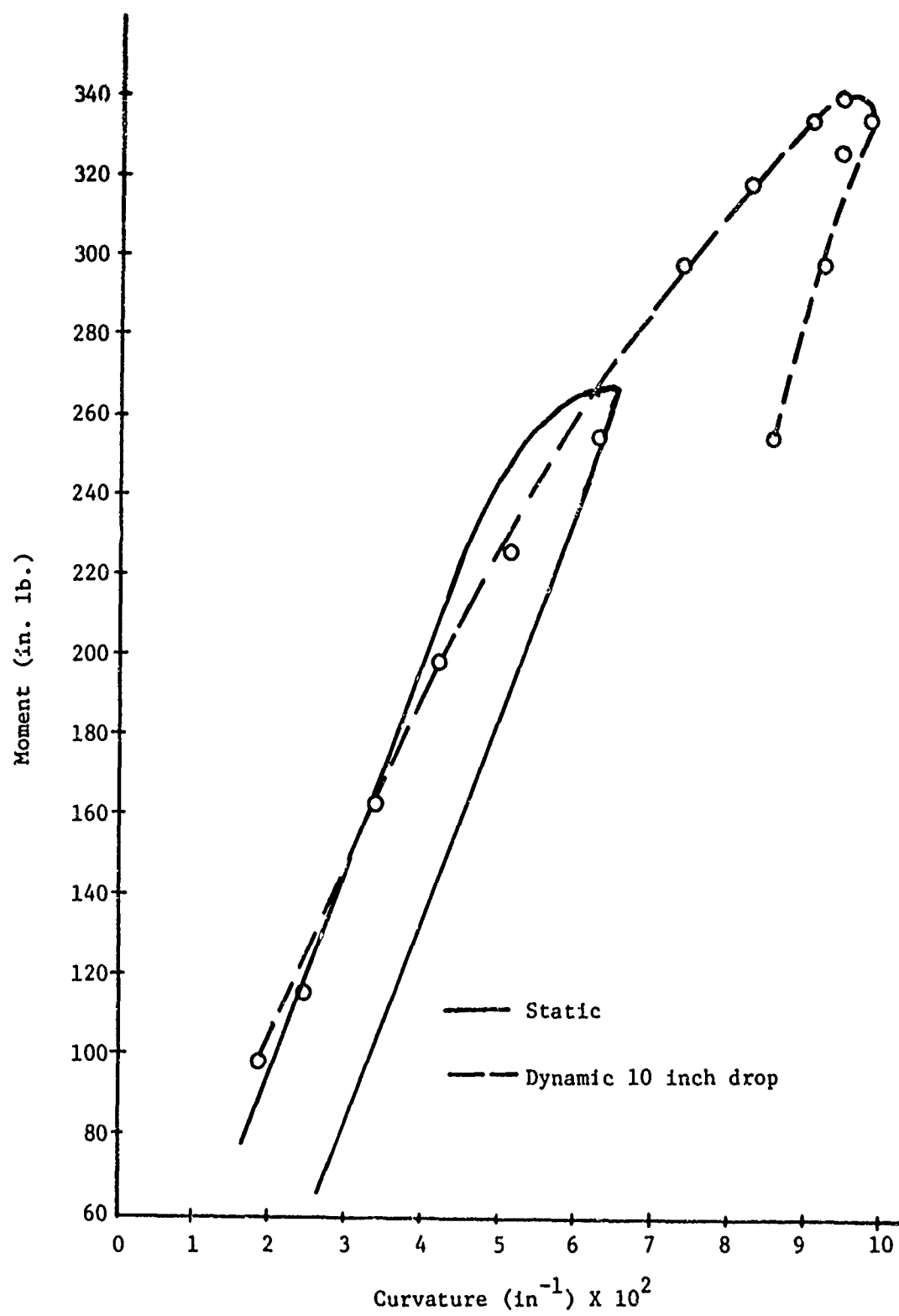


Fig. 4 Static and Dynamic Moment vs. Curvature

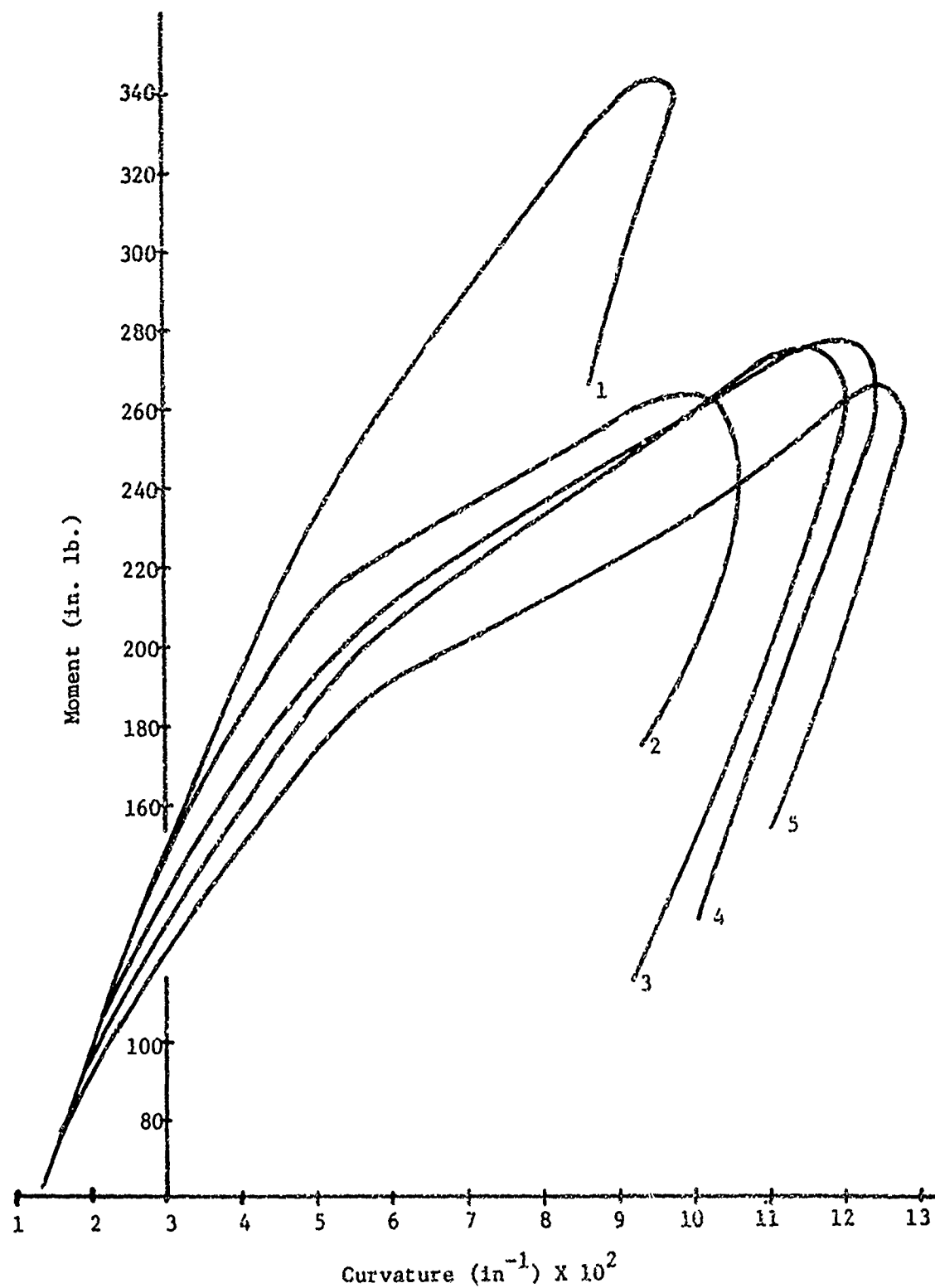


Fig. 5 Dynamic Moment vs. Curvature ~ Repeated 10 inch Drops

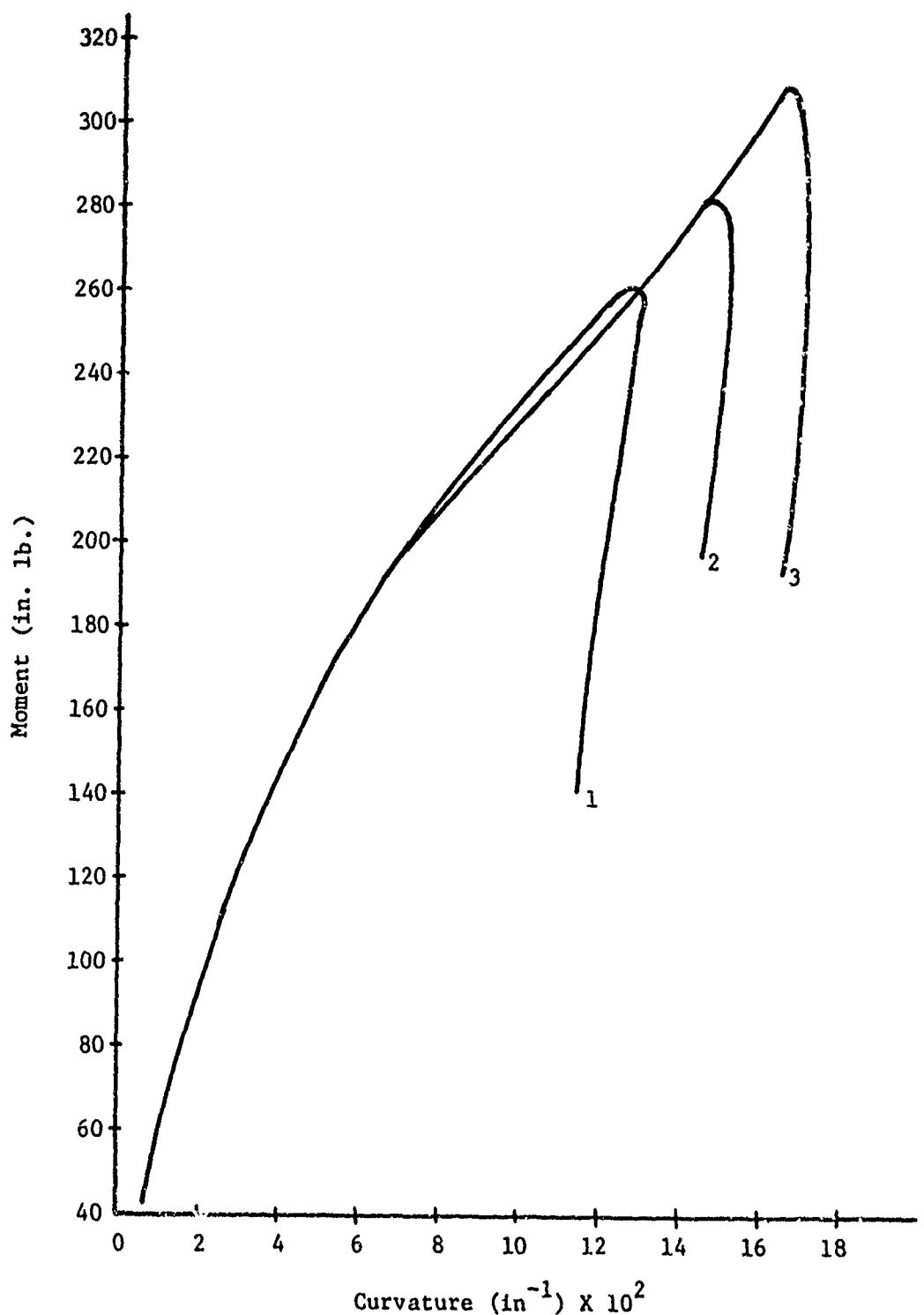


Fig. 6 Dynamic Moment vs. Curvature - Successive 10, 12 and 14 inch Drops

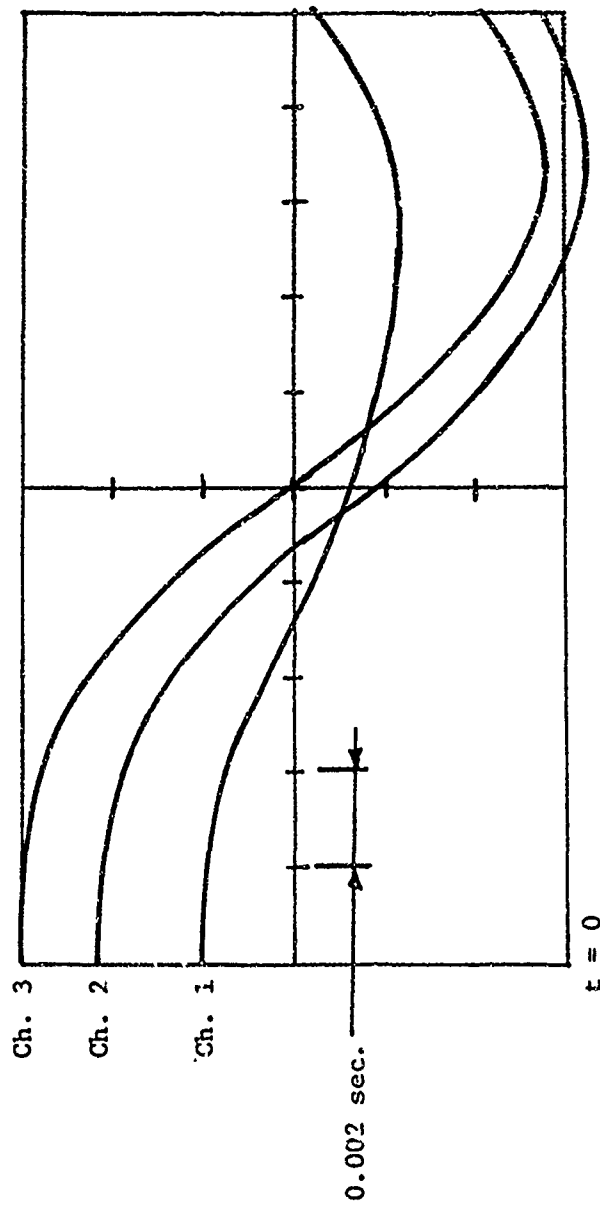


Fig. 7 Strain Records vs. Time on Oscilloscope

## II. Relationship Between Moment-Curvature and Stress-Strain Constitutive Relationships

W. Vogel and V. H. Neubert

Much basic study has been devoted to the behavior of materials in simple tension or compression. Tests have been performed which have led to constitutive relationships including rate effects. The purpose here is to attempt to develop the moment-curvature relationship for a beam based on an assumed stress-strain relationship. The development follows that presented first by Vogel<sup>(6)</sup>. We assume that the total strain rate  $\dot{\epsilon}$  could be represented as the sum of  $\dot{\epsilon}'$ , the elastic strain rate, and  $\dot{\epsilon}''$ , the plastic strain rate, that is

$$\dot{\epsilon} = \dot{\epsilon}' + \dot{\epsilon}'' \quad (16)$$

In Figure 8 a cantilever beam carrying a concentrated load is shown. If the beam is long and slender, it is assumed that shear effects may be neglected with regard to effect on yielding.

Vogel<sup>(6)</sup> assumed that the total stress  $\sigma$  in the plastic region, of area  $A_2$ , could be represented by

$$\sigma = \sigma_{st} + b\dot{\epsilon}'' \quad (17)$$

The moment  $M_p$  due to stress in the plastic region, if the beam is

symmetrical with respect to the neutral axis is

$$M_p = \int_{A_2} \sigma w(y) y dy \quad (18)$$

where  $w(y)$  is the width of the cross-section.

Using (17) in (18)

$$M_p = \int_{A_2} \sigma_{st} w(y) y dy + b \int \dot{\varepsilon}'' w(y) y dy \quad (19)$$

The first integral is the contribution to  $M_{st}$  due to the stresses on  $A_2$ . In the second integral, let  $\dot{\varepsilon}'' = \dot{\varepsilon} - \dot{\varepsilon}'$  from (16).

$$M_p = (M_{st})_{A_2} + b \int_{A_2} (\dot{\varepsilon} - \dot{\varepsilon}') w(y) y dy \quad (20)$$

If plane sections before bending remain plane after bending  $\dot{\varepsilon} = ky$ , with  $k$  the curvature at the cross-section. Also, we assume  $\dot{\varepsilon}' = \frac{\dot{\sigma}}{E}$  and (20) becomes

$$M_p = (M_{st})_{A_2} + b k I_{A_2} - \frac{b (\dot{M})_{A_2}}{E} \quad (21)$$

On the elastic region  $A_1$ ,  $\sigma = \sigma_{st}$  so the contribution to the moment  $M_s$  due to stresses on  $A_2$  would be

$$M_s = (M_{st})_{A_1} \quad (22)$$

The total moment is  $M = M_p + M_s$ , or

$$M = M_{st} + b \dot{k} I_{A_2} - \frac{b \dot{M}_{A_2}}{E} \quad (23)$$

$$\text{or} \quad \dot{k} = \frac{\dot{M}_{A_2}}{EI_{A_2}} + \frac{1}{bI_{A_2}} (M - M_{st}) \quad (24)$$

As the bending increases  $A_2 \rightarrow A$  as  $A_1 \rightarrow 0$  where  $A$  is the total area of the cross-section, resulting in

$$\dot{k} = \frac{\dot{M}}{EI} + \frac{1}{bI} (M - M_{st}) \quad (25)$$

Although there are assumptions in the derivation of Equation (24) which are open to question, the form has some logic. Written in the form

$$EI_{A_2} \dot{k} = \dot{M}_{A_2} + \frac{E}{b} (M - M_{st}) \quad (26)$$

it is clear that when the section is entirely elastic,  $I_{A_2} = 0$  and

$\dot{M}_{A_2} = 0$  resulting in  $M = M_{st}$ .

Comparing Equation (25) with Equation (1) and Equation (5) in Part I, it is clear that  $C = \frac{E}{b} = REI$ . If this is true, the results of the present study may be extended directly to beams of other cross-sections without further tests. An investigation is in progress to check this result.

Equation (25) may be derived in a more direct way if one uses an equation presented by Malvern<sup>(4)</sup> as follows:

$$\dot{c} = \frac{\dot{\sigma}}{E} + \frac{1}{b} [\sigma - \sigma_{st}] \quad (27)$$

Since this applies to the complete loading range, we need not distinguish between elastic and plastic regions. Letting  $\dot{\epsilon} = \dot{y}/k$ , we multiply (27) by  $y$  and integrate over the cross-section, arriving directly at the relationship

$$I \dot{k} = \frac{\dot{M}}{E} + \frac{1}{b} [M - M_{st}]. \quad (28)$$

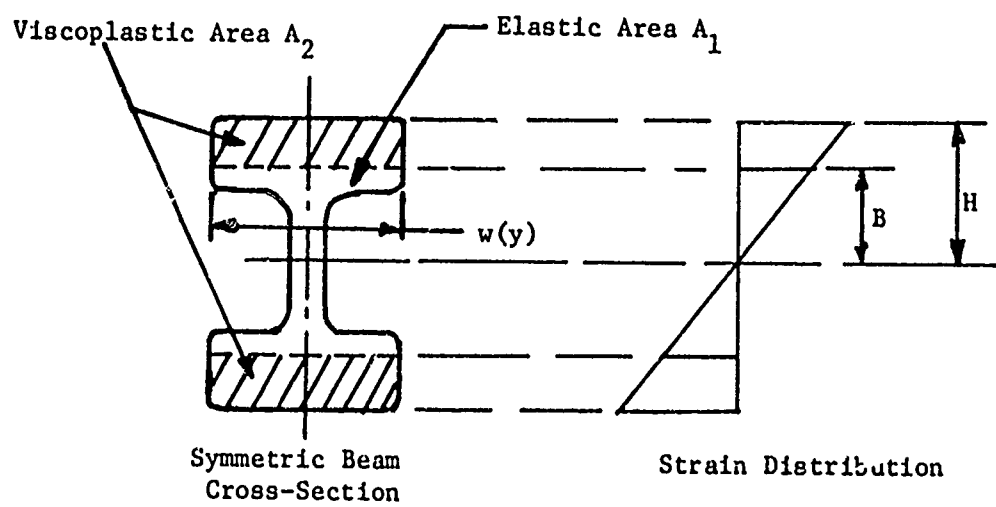
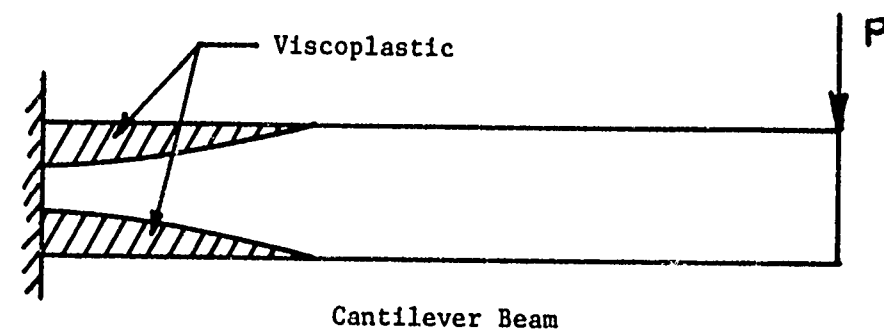


Fig. 8. Cantilever Beam With Viscoplastic Region

III. Theoretical Response of an Idealized  
Viscoplastic Cantilever Beam

R. Weiss and V. H. Neubert

Introduction

One of the goals of the present work is to arrive at equations suitable for design analysis of structures loaded dynamically into the plastic range. For many existing computer programs using finite elements, it is easy to include a new element once its behavior is stated in the form of a transfer matrix, a flexibility matrix, or a stiffness matrix. With this in mind, the transfer matrix and the stiffness matrix were presented in reference (1) for a viscoplastic beam element which behaves according to the equation discussed in Parts I and II of this report:

$$\dot{k} = \frac{\dot{M}}{EI} + R(M - M_{st}) \quad (29)$$

To retain a linear form of the differential equation it was assumed that  $M_{st}$  could be represented in a piecewise linear manner, the simplest form being

$$M_{st} = S_1 k \quad \text{for } k < k_y \quad (30)$$

$$M_{st} = M_y + S_2 (k - k_y) \quad \text{for } k \geq k_y$$

which is shown in Figure 9. A brief discussion was presented in reference (1) of the form of solution of the differential equation of a cantilever beam under dynamic loading assuming that Equation (29) applies for the entire beam length.

To gain experience with the analysis based on the matrix equations presented in reference (1), which are valid in both elastic and plastic ranges, a computer program has been written for the exact solution of a two-segment cantilever carrying a tip mass as shown in Figure 10. The need for two segments arises from the two ranges of curvature in the bi-linear form of  $M_{st}$  as given in Equation (30). In order to account for the  $i^{th}$  beam segment in the constitutive relationship, an additional subscript is now inserted, so that Equation (30) became

$$M_{st} = S_{il} k \quad c \leq k \leq k_y \quad (31)$$

$$M_{st} = M_y + S_{i2} (k - k_y) \quad k \geq k_y$$

The first subscript is the beam segment number, the second subscript the loading range on the linearized  $M_{st}$  versus  $k$  range. With the bi-linear curve used here,  $S_{il}$  implies the elastic range and  $S_{i2}$  the plastic range.

The loading to the beam of Figure 10 was taken as a base acceleration  $\ddot{y}_o(t)$  of a triangular form as shown in Figure 11. This approximates the pulse obtained from the Barry Shock Machine at the Naval Research Laboratory as discussed in reference (1).

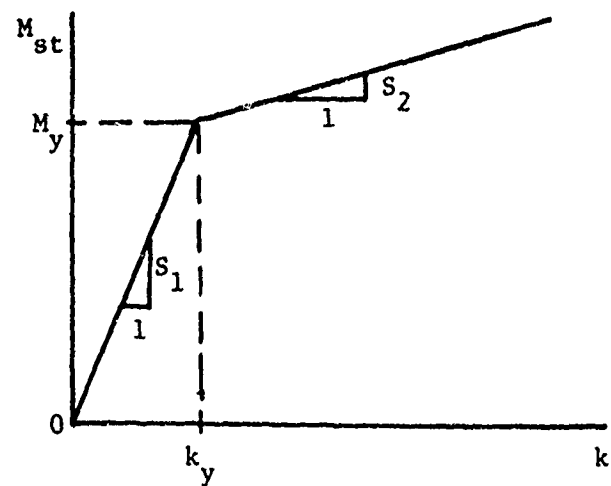
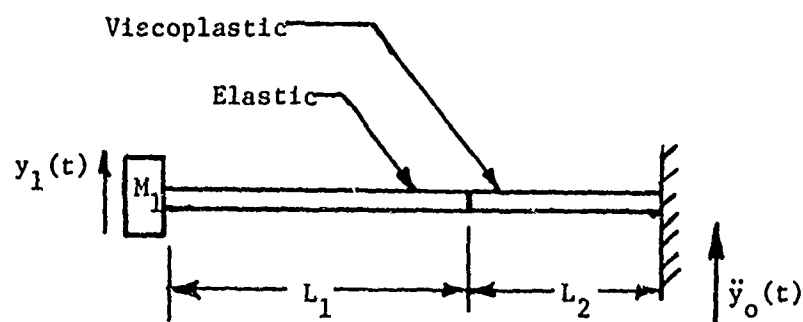
Fig. 9 Bi-linear Static Moment vs.  $k$ 

Fig. 10 Two-Segment Viscoplastic Beam

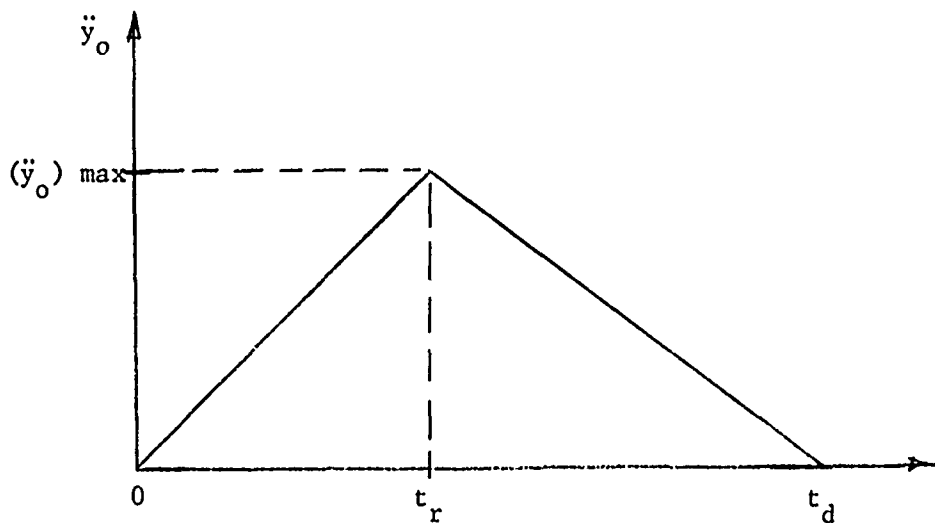


Fig. 11  $\ddot{y}_o$  vs.  $t$

As the beam is initially loaded  $L_1 = L$  the total beam length and  $L_2 = 0$ . As the loading increases the moment at the base would first exceed  $M_y$  and a plastic "hinge" begin to develop. If at this time a plastic hinge is inserted having a finite length  $L_2$ , the moment at the elastic-plastic interface between beam segments 1 and 2 would be slightly less than  $M_y$ , but would continue to increase as the dynamic loading increases. As soon as the moment at the interface equals  $M_y$ ,

the length  $L_2$  would be increased. The rate at which the interface moves depends on the material and the loading rate. To gain experience with the effect of hinge length on beam response, hinges of various lengths  $L_2$  were used and their lengths kept constant throughout the analysis. This is equivalent to analyzing a beam made of two materials where the material in segment 1 has such a high yield that it always remains elastic. In later analysis this limitation is removed so that  $L_2 = L_2(t)$ .

#### Equations of Motion

The equation of motion of the elastic-plastic cantilever beam in terms of displacement  $y_1$  of the tip mass relative to the base is

$$A_1 \ddot{y}_1 + A_2 \ddot{y}_1 + A_3 \dot{y}_1 + A_4 y_1 = B_1 \ddot{y}_0 + B_2 \ddot{y}_0 + B_3 (-M_y + S_{22} k_y) \quad (32)$$

where

$$A_1 = 1$$

$$D A_2 = L_1^3 R S_{21} S_{22} + 3L_1^2 L_2' R S_{11} S_{21} + 3L_1 L_2^2 R S_{11} S_{21} + L_2^3 R S_{11} S_{21}$$

$$D A_3 = \frac{3 S_{11} S_{21}}{m_1}$$

$$D A_4 = \frac{3R S_{11} S_{21} S_{22}}{m_1}$$

$$B_1 = -A_1$$

$$B_2 = -A_2$$

$$D B_3 = \frac{3L_2 (L_1 + L_2/2) R S_{11} S_{21}}{m_1}$$

$$B_3^* = B_3 (-M_y + S_{22} k_y)$$

$$D = L_1^3 S_{21} + 3L_1^2 L_2 S_{11} + 3L_1 L_2^2 S_{11} + L_2^3 S_{11}$$

For the prescribed pulse, the solution for  $y_1$  can be expressed exactly during the three stages of loading in Figure 11, the rise era, the decay era, and the free vibration era. The solutions written below are in terms of generalized initial conditions occurring at yield time  $t_y$  at the onset of development of the plastic hinge.

For the rise era,  $0 \leq t \leq t_d$ , the initial conditions are

$$y_1(t = t_y) = y_{1r}$$

$$\dot{y}_1(t = t_y) = \dot{y}_{1r} \quad (33)$$

$$\ddot{y}_1(t = t_y) = \ddot{y}_{1r}$$

The solution is

$$y_1(t) = c_1 e^{r_1(t - t_y)} + e^{r_2(t - t_y)} [c_2 \cos r_3(t - t_y)] \\ + c_3 \sin r_3(t - t_y) + \frac{\ddot{y}_0 \max}{A_4 t_r} \left[ B_1 + B_2 t - \frac{A_3 B_2}{A_4} \right] + \frac{B_3^*}{A_4} \quad (34)$$

$$\begin{aligned}
 c_1 &= \frac{1}{r_s^2} \left\{ \left( r_2^2 + r_3^2 \right) G_{1r} - 2r_2 G_{2r} + \ddot{y}_{1r} \right\} \\
 c_2 &= \frac{1}{r_s^2} \left\{ r_1(r_1 - 2r_2) G_{1r} + 2r_2 G_{2r} - \ddot{y}_{1r} \right\} \\
 c_3 &= \frac{1}{r_3 r_s^2} \left\{ r_1 \left( r_2^2 - r_3^2 - r_1 r_2 \right) G_{1r} + \left( r_1^2 - r_2^2 + r_3^2 \right) G_{2r} \right. \\
 &\quad \left. + (r_2 - r_1) \ddot{y}_{1r} \right\}
 \end{aligned}$$

$$r_s^2 = (r_1 - r_2)^2 + r_3^2$$

$$\begin{aligned}
 G_{1r} &= y_{1r} - \frac{(\ddot{y}_o)_{\max}}{A_4 t_r} \left( B_1 + B_2 t_y - \frac{A_3 B_2}{A_4} \right) - \frac{B_3^*}{A_4} \\
 G_{2r} &= \dot{y}_{1r} - \frac{(\ddot{y}_o)_{\max}}{A_4 t_r}
 \end{aligned}$$

For the decay era, the initial conditions are used in the form of (33), except the subscript is d instead of r. The solution is:

$$\begin{aligned}
 y_1(t) &= D_1 e^{r_1(t - t_y)} + e^{r_2(t - t_y)} [D_2 \cos r_3(t - t_y) \\
 &\quad + D_3 \sin r_3(t - t_y)] - \frac{(\ddot{y}_o)_{\max}}{A_4(t_d - t_r)} \left[ B_1 - B_2(t_d - t) - \frac{A_3 B_2}{A_4} \right] \\
 &\quad + \frac{B_3^*}{A_4}
 \end{aligned} \tag{35}$$

$$\begin{aligned}
 D_1 &= \frac{1}{r_s^2} \left\{ \left( r_2^2 + r_3^2 \right) G_{1d} - 2r_2 G_{2d} + \ddot{y}_{1d} \right\} \\
 D_2 &= \frac{1}{r_s^2} \left\{ r_1(r_1 - 2r_2) G_{1d} + 2r_2 G_{2d} - \ddot{y}_{1d} \right\} \\
 D_3 &= \frac{1}{r_3 r_s^2} \left\{ r_1 \left( r_2^2 - r_3^2 - r_1 r_2 \right) G_{1d} + \left( r_1^2 - r_2^2 + r_3^2 \right) G_{2d} \right. \\
 &\quad \left. + (r_2 - r_1) \dot{y}_{1d} \right\} \\
 G_{1d} &= y_{1d} + \frac{(\ddot{y}_o)_{\max}}{A_4(t_d - t_r)} \left[ B_1 - B_2(t_d - t_y) - \frac{A_3 B_2}{A_4} \right] - \frac{B_3^*}{A_4} \\
 G_{2d} &= \dot{y}_{1d} + \frac{(\ddot{y}_c)_{\max} B_2}{A_4(t_d - t_r)}
 \end{aligned}$$

After the pulse is terminated, for  $t \geq t_d$ , the initial conditions are used as in (33) with an a subscript instead of an r. The solution is:

$$\begin{aligned}
 y_1(t) &= E_1 e^{r_1(t - t_y)} + e^{r_2(t - t_y)} [E_2 \cos r_3(t - t_y) \\
 &\quad + E_3 \sin r_3(t - t_y)] + \frac{B_3^*}{A_4} \tag{36}
 \end{aligned}$$

$$\begin{aligned}
 E_1 &= \frac{1}{r_s^2} \left\{ \left( r_2^2 + r_3^2 \right) \left[ y_{1a} - \frac{B_3^*}{A_4} \right] - 2r_2 \dot{y}_{1a} + \ddot{y}_{1a} \right\} \\
 E_2 &= \frac{1}{r_s^2} \left\{ r_1(r_1 - r_2) \left[ y_{1a} - \frac{B_3^*}{A_4} \right] + 2r_2 \dot{y}_{1a} - \ddot{y}_{1a} \right\} \\
 E_3 &= \frac{1}{r_3 r_s^2} \left\{ r_1 \left( r_2^2 - r_3^2 - r_1 r_2 \right) \left[ y_{1a} - \frac{B_3^*}{A_4} \right] + \left( r_1^2 - r_2^2 + r_3^2 \right) \dot{y}_{1a} \right. \\
 &\quad \left. + (r_2 - r_1) \ddot{y}_{1a} \right\}
 \end{aligned}$$

#### Beams Studied Using a Constant $L_2$

To more effectively study the effects of key parameters such as the material constant R and plastic hinge length  $L_2$ , a computer program was written which calculates tip displacement, velocity and acceleration, base moment and curvature, and the time rates of change of both base moment and base curvature at various intervals of time until the dynamic moment at the base equals the yield value. When the beam has yielded at the base, a plastic hinge is inserted at time  $t_y$ , and again the response variables calculated, including the moment at the elastic-plastic interface. Realistic values for the base acceleration were obtained from reference (1), Figure 11, page 110. The values used are:

$$\ddot{y}_o \text{ max} = 100 \text{ g}$$

$$m_1 = 0.012 \text{ #sec}^2/\text{in}$$

$$t_r = 0.004 \text{ sec.}$$

$$S_{11} = S_{21} = 5000 \text{ #in}^2$$

$$t_d = 0.006 \text{ sec.}$$

$$S_{22} = 500 \text{ #in}^2$$

$$L = L_1 + L_2 = 5 \text{ inches}$$

Values of yield moment (247 in $\cdot$ lb) and yield curvature (.05 in $^{-1}$ ) were gotten from reference (3).

In Figures 12-16, the tip displacement versus time is shown for various values of R and L<sub>2</sub>. It was hoped that some of the response variables might be found to be relatively insensitive to hinge length and that this would simplify design analysis. To date, it has been found that hinge length is quite important. On each figure one example curve is also shown for R = 1 in which the hinge was inserted at t = 0. The effect on prediction of maximum displacement is an error of 20%. In Figures 17-20, the moment M<sub>2</sub> at the elastic-plastic interface is plotted versus time. As soon as this moment reaches the yield moment the hinge would be extended if both beam segments were of the same value. The main use for the curves at present is that they give an analyst an idea of the rate of propagation of a hinge for various values of L<sub>2</sub> and R.

#### Results Using a Variable L<sub>2</sub>

The next step was to use a variable viscoplastic hinge length L<sub>2</sub>. For the present examples, L<sub>2</sub> was incremented in 0.05 inch intervals. The process was as follows. As in the previous examples, the moment at the support was monitored. As soon as it reached the yield moment M<sub>y</sub>, a viscoplastic hinge 0.05 inches long was inserted. The moment M<sub>2</sub> at the elastic-viscoplastic interface would at that instant be slightly less than M<sub>y</sub>. The timewise variation in M<sub>2</sub> was then monitored and, as soon as M<sub>2</sub> = M<sub>y</sub>, the hinge was lengthened by .05 inches. This process was continued to allow the hinge to develop as required by conditions

at the interface. The effect of the incrementing procedure and its relation to convergence is being studied further.

In Figure 21, the effect on the tip displacement  $y_1(t)$  of having a variable hinge length  $L_2$  is indicated for  $R = 0.1$ . The solution for  $L_2$  a variable is compared with those previously discussed for  $L_2 = 0.05$ , 0.25, and 0.50 inches. It can be seen that the variable hinge solution is very close to that for  $L_2 = 0.50$  inches. In Figure 22 a similar set of curves is shown for  $R = 1$ . Here the more exact variable hinge solution is closest to that for  $L_2 = 0.25$  inches.

In Figure 23 the variation of  $L_2$  with time is plotted for  $R = 0.1$  and 1. For  $R = 0.1$ , the hinge reaches its final length of 0.5 inches in a relatively short time. For  $R = 1$ , the hinge spreads less rapidly and reaches a total length of 0.3 inches. It is interesting to note that these total hinge lengths are approximately the same as the constant lengths whose solutions for  $y_1$  on Figures 21 and 22 most closely agreed with those for variable hinge length as discussed in the previous paragraph. This may have some practical utility, since it is easier to solve for response using a constant hinge length. However, at present we have no way to predict the hinge length without carrying out the more exact solution.

The variation of moment  $M_2$  with time at the moving interface is shown in Figure 24 for  $R = 0.1$  and 1. For  $R = 0.1$ , the hinge develops to its full length rapidly and then the interface moment begins to decrease. For  $R = 1$ , a cyclic decrease and subsequent increase in moment each time the length of the hinge is incremented is much more pronounced, indicating that an increment length smaller than 0.05 inches should be used.

Summary and Conclusions

The purpose of this part of the report has been to present some results from a computer program for the exact analysis of the viscoplastic beam under shock. The displacements calculated using hinges of constant length  $L_2$  and variable length  $L_2$  should be upper bounds, because elastic unloading and shortening of the hinge have not been accounted for in the curves presented. The computer analysis can easily take these effects into account. One of the final goals of this theoretical study is to investigate the effects of yielding of supports and foundations on design shock spectra.

In the overall study of development of yielding and failure criteria, the importance of experimental data can not be overemphasized. The constitutive relationship postulated in Part II accounting for dependence on cross-sectional shape of a beam needs to be checked experimentally, and modified, if necessary. Different cross-sectional shapes of various practical materials need to be investigated. In general, the ability to calculate using the digital computer presently exceeds the amount of experimental data available for guidance of analysis.

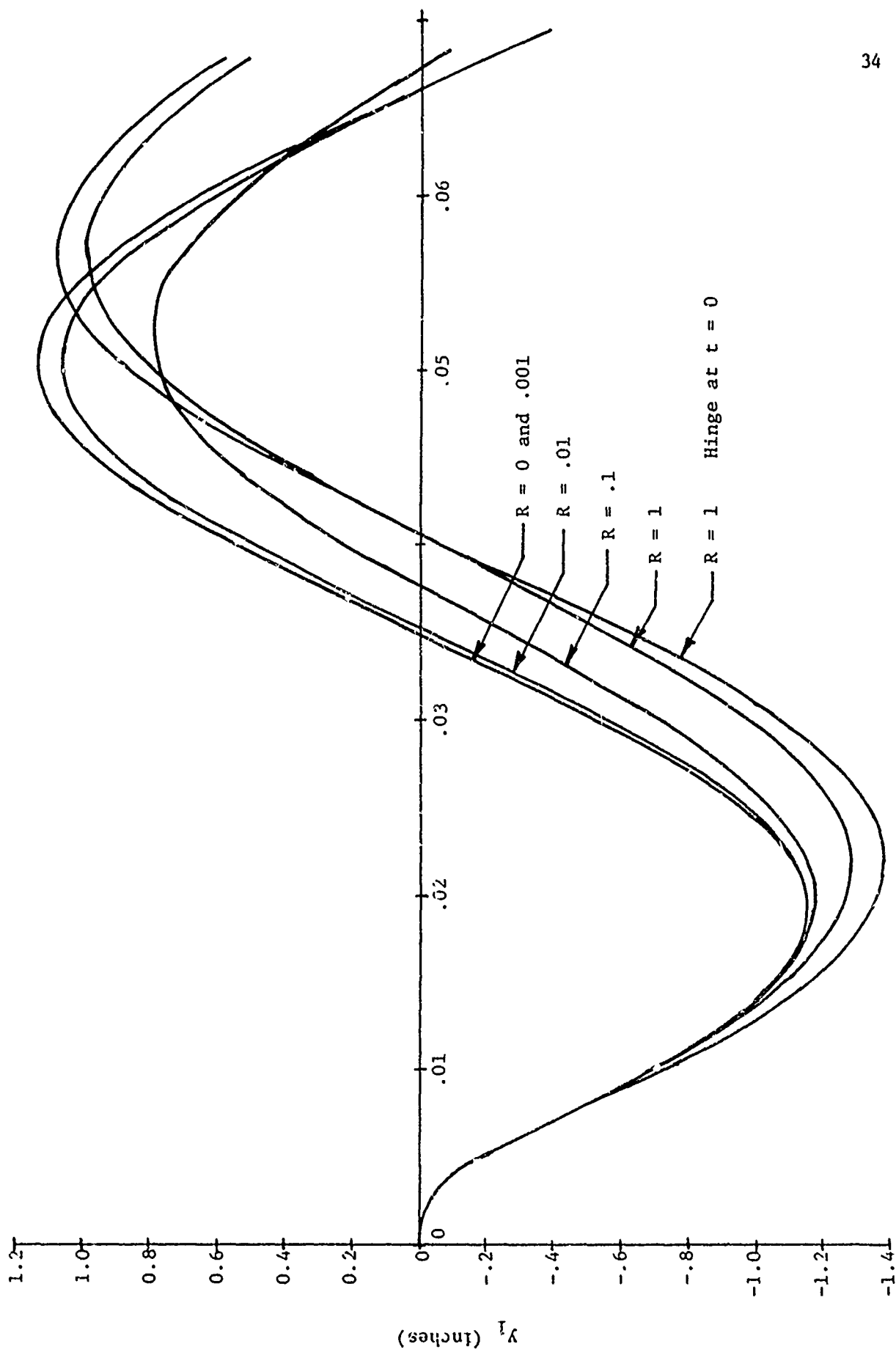


Fig. 12  $y_1$  vs.  $t$ , Various  $R$ ,  $L_2 = 0.05$  inches

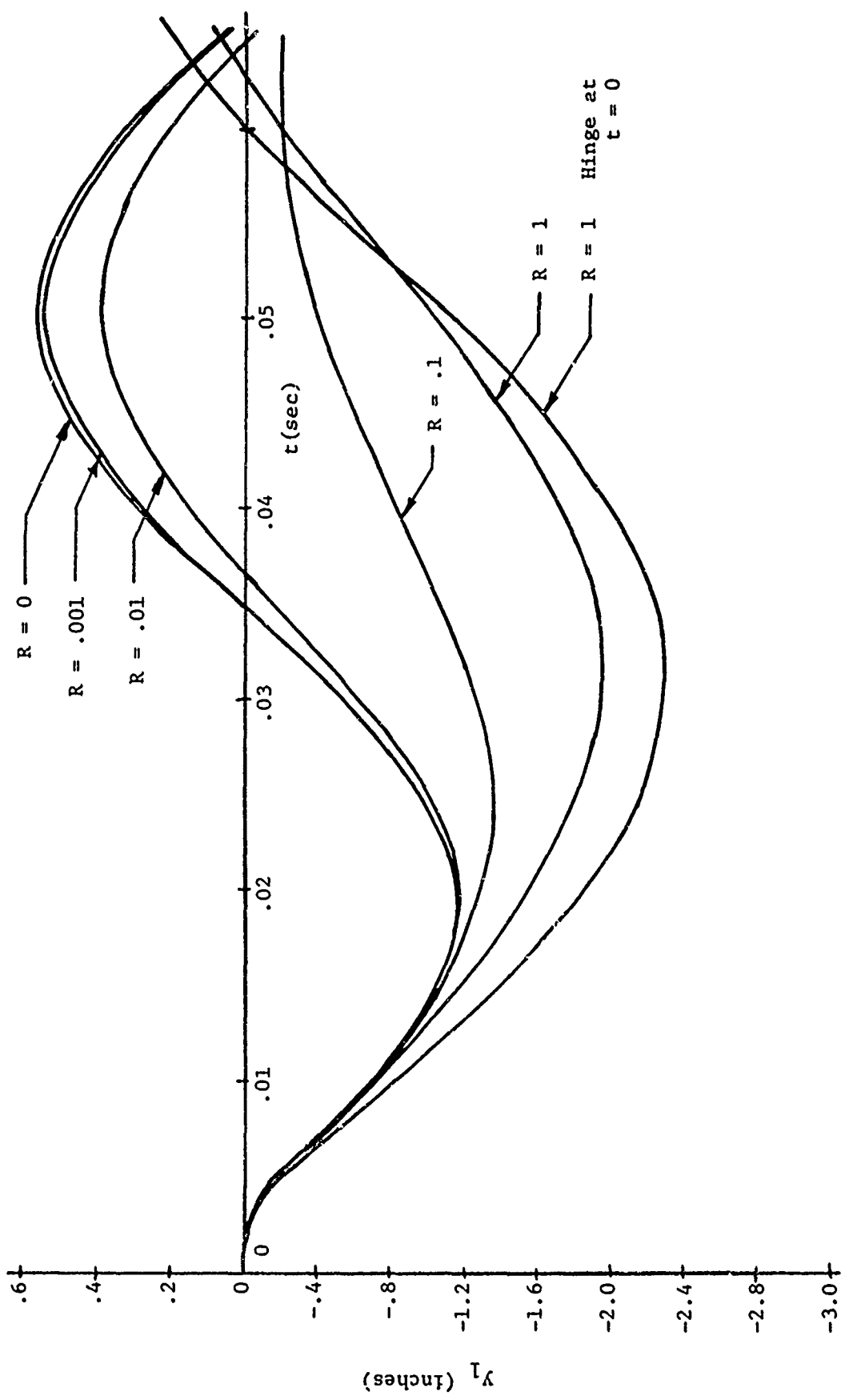


Fig. 13  $y_1$  vs.  $t$ , Various  $R$ ,  $L_2 = 0.25$  inches

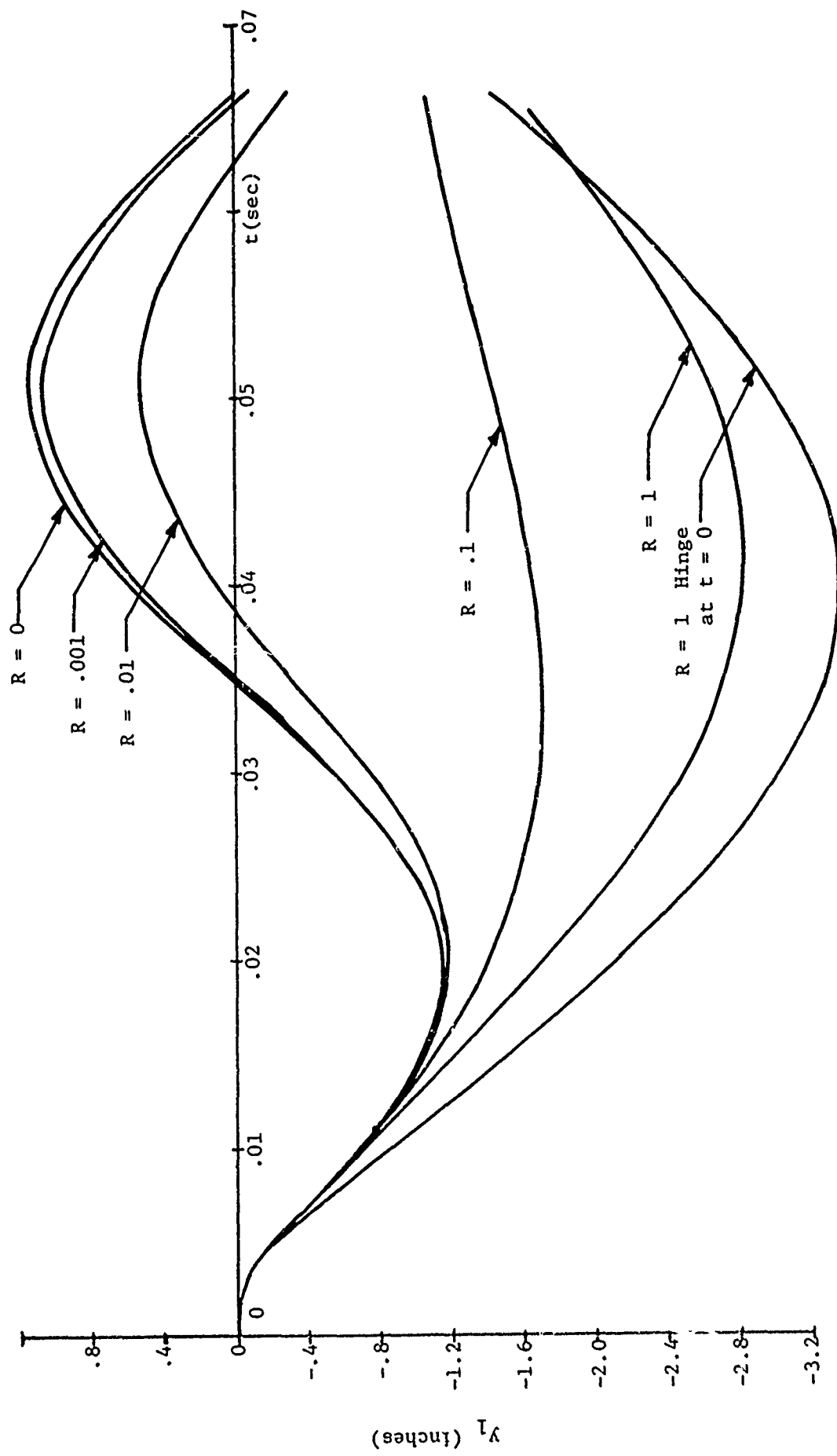


Fig. 14  $y_1$  vs.  $t$ , Various  $R$ ,  $L_2 = 0.50$  inches

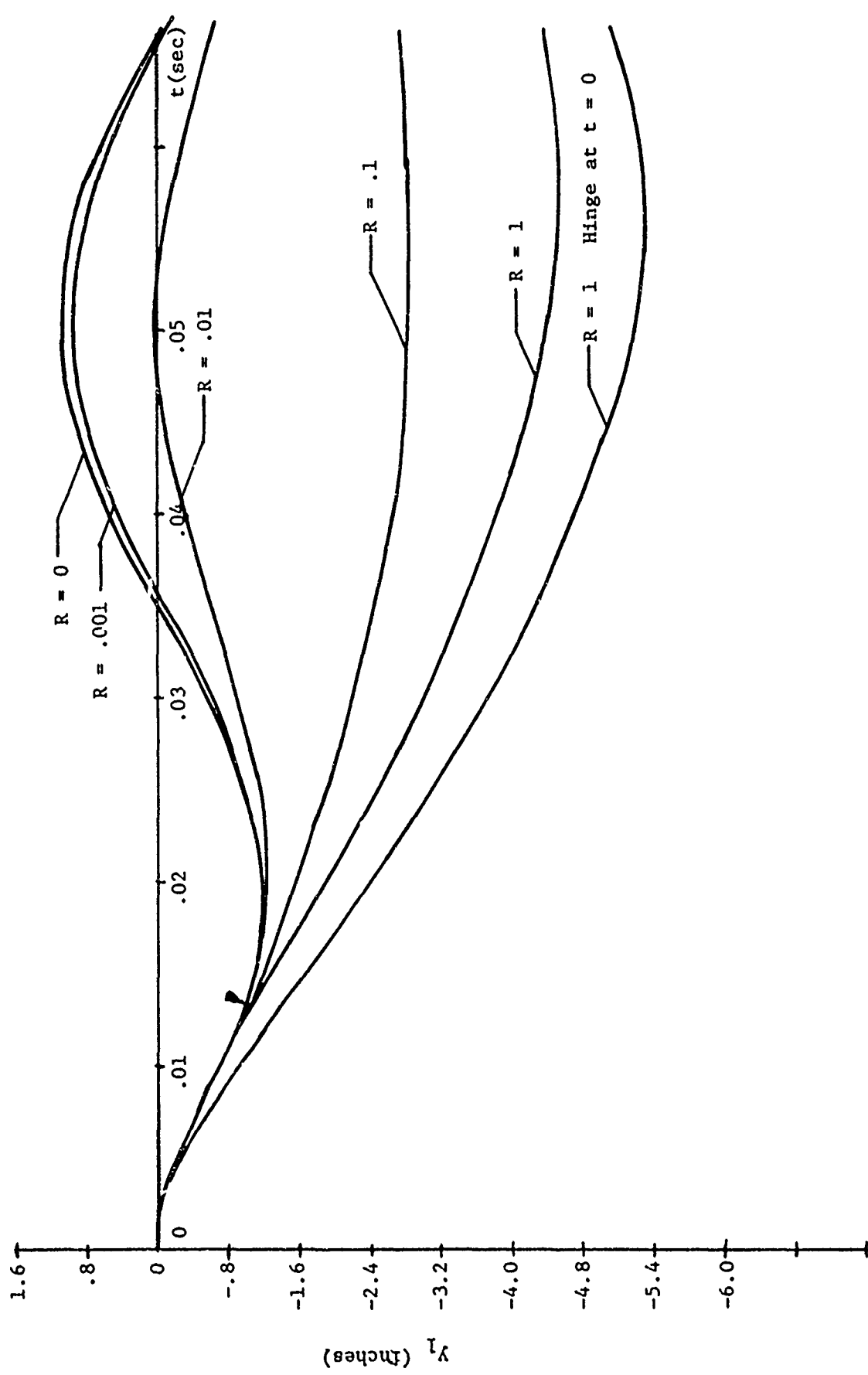


Fig. 15  $y_1$  vs.  $t$ , Various  $R$ ,  $L_2 = 1.0$  inches

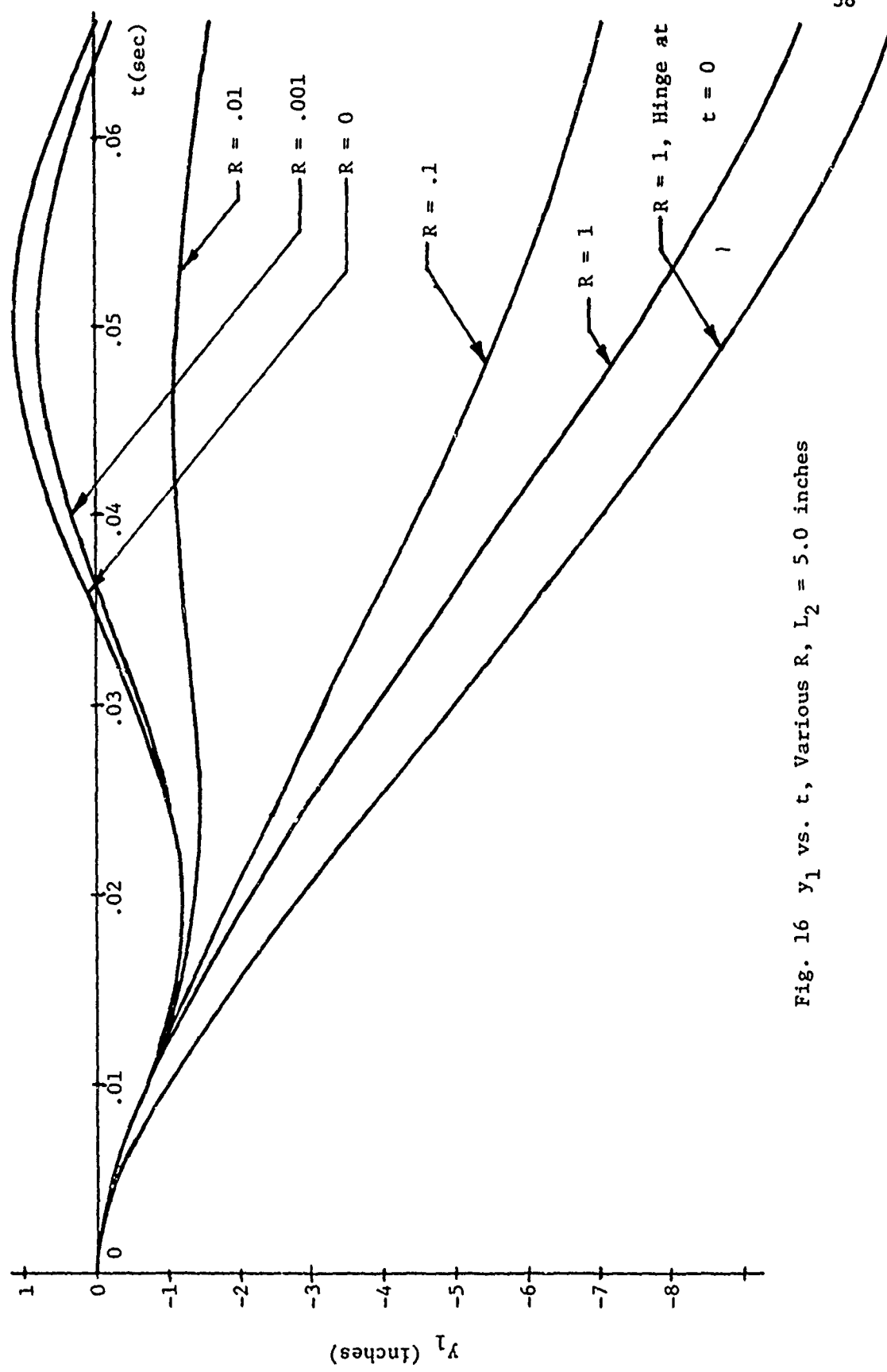


Fig. 16  $y_1$  vs.  $t$ , Various  $R$ ,  $L_2 = 5.0$  inches

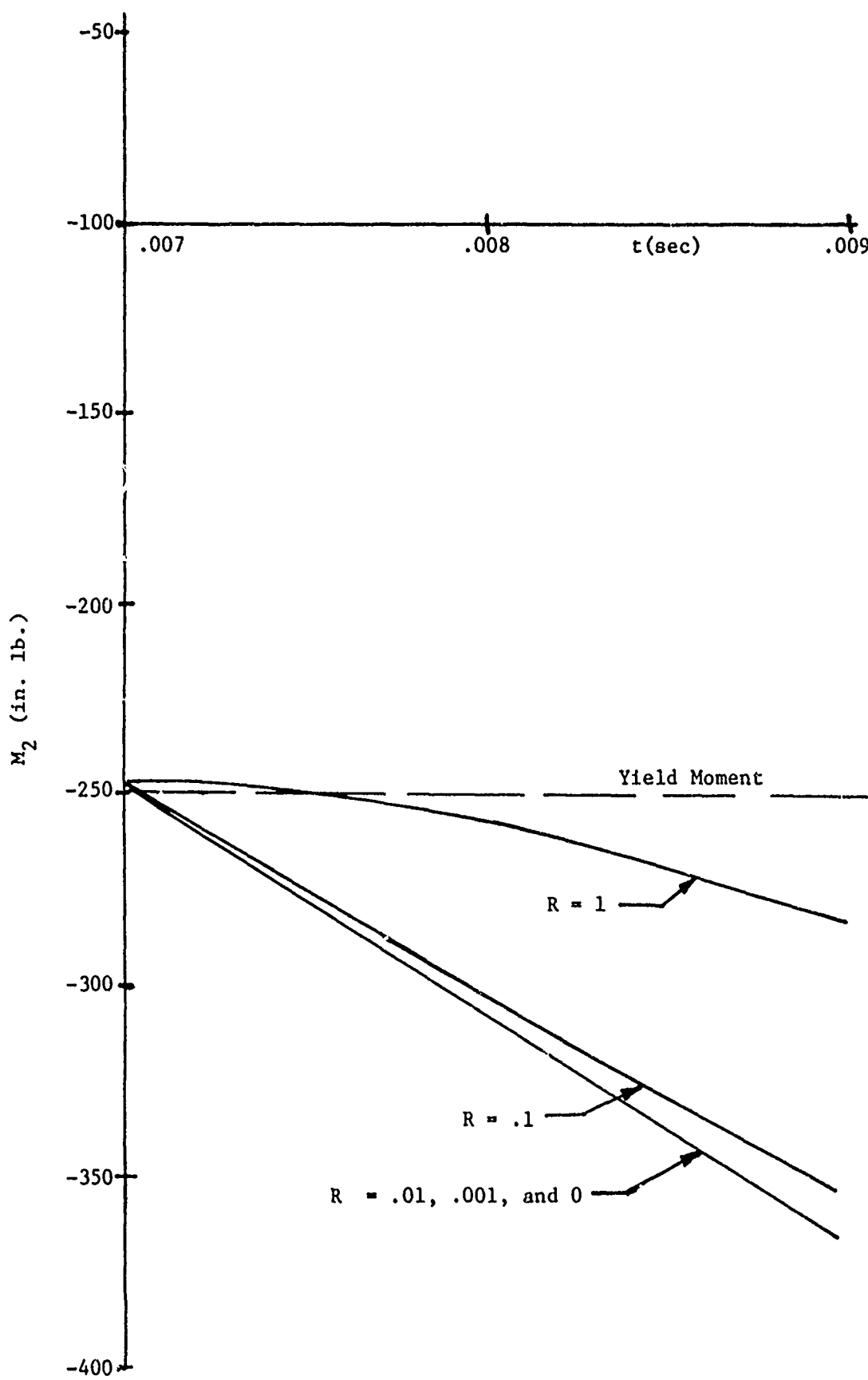


Fig. 17  $M_2$  vs.  $t$ , Various  $R$ ,  $L_2 = 0.05$  inches

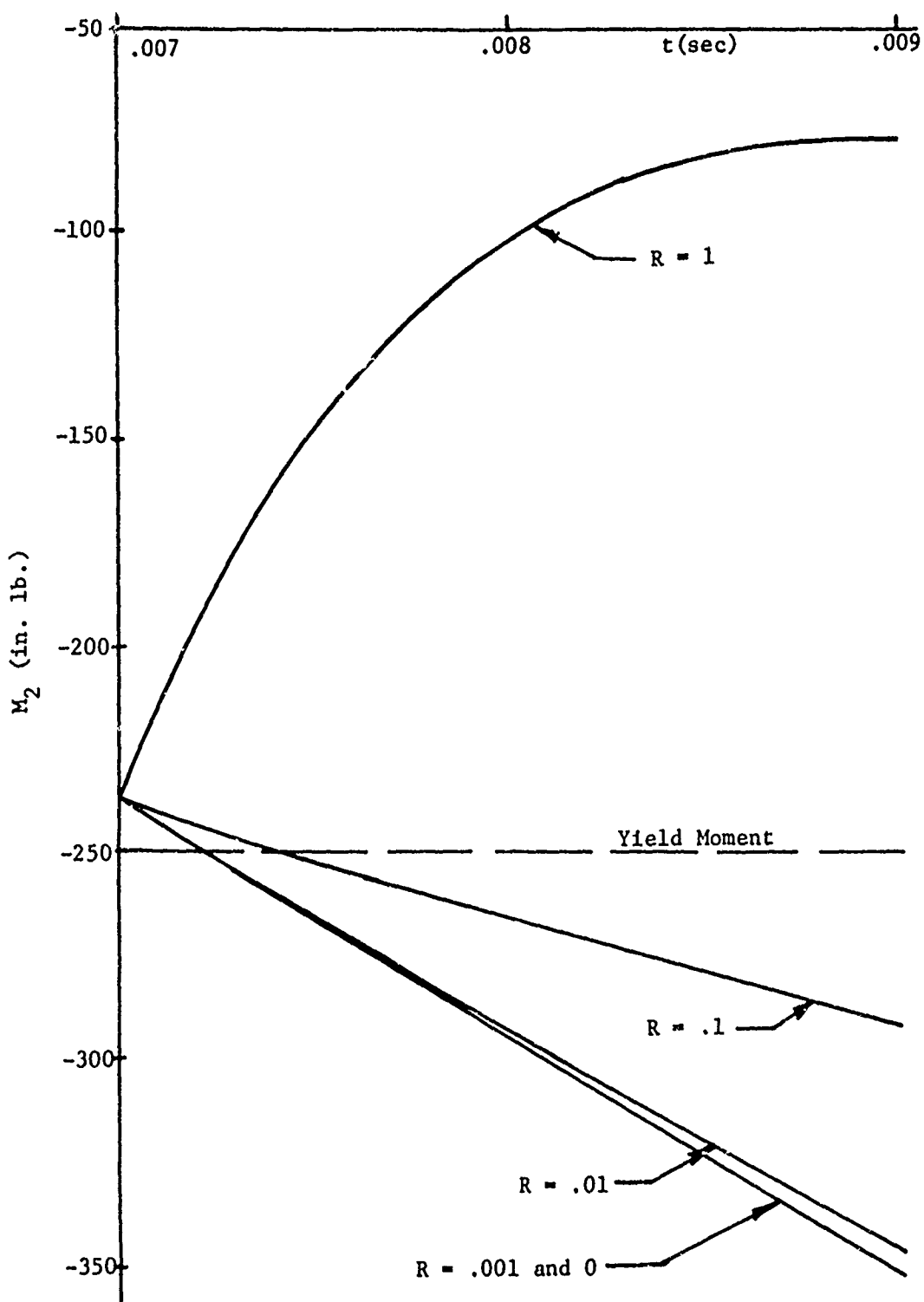


Fig. 18  $M_2$  vs.  $t$ , Various  $R$ ,  $L_2 = 0.25$  inches

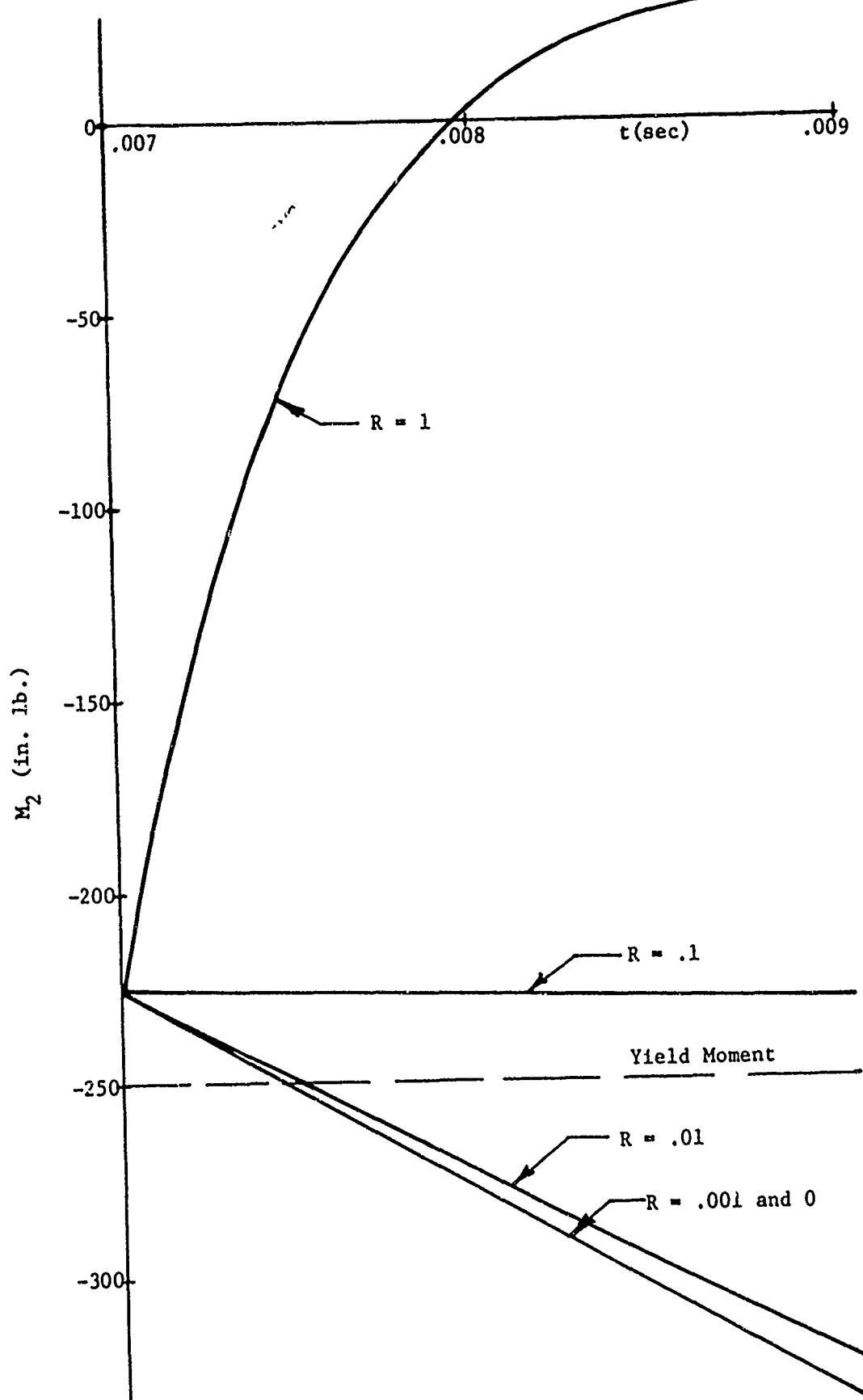
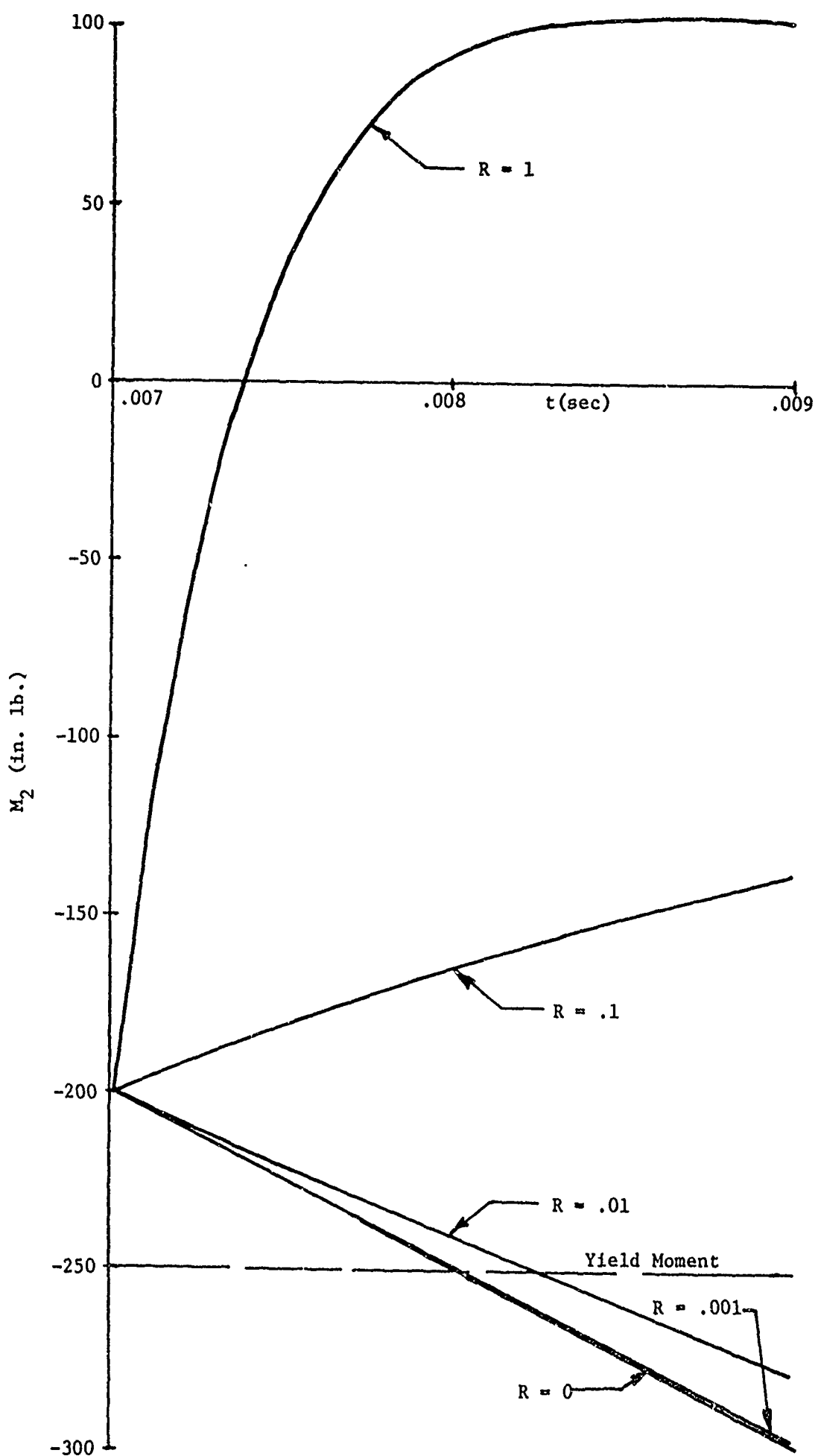


Fig. 19  $M_2$  vs.  $t$ , Various  $R$ ,  $L_2 = 0.5$  inches

Fig. 20  $M_2$  vs.  $t$ , Various  $R$ ,  $L_2 = 1.0$  inches

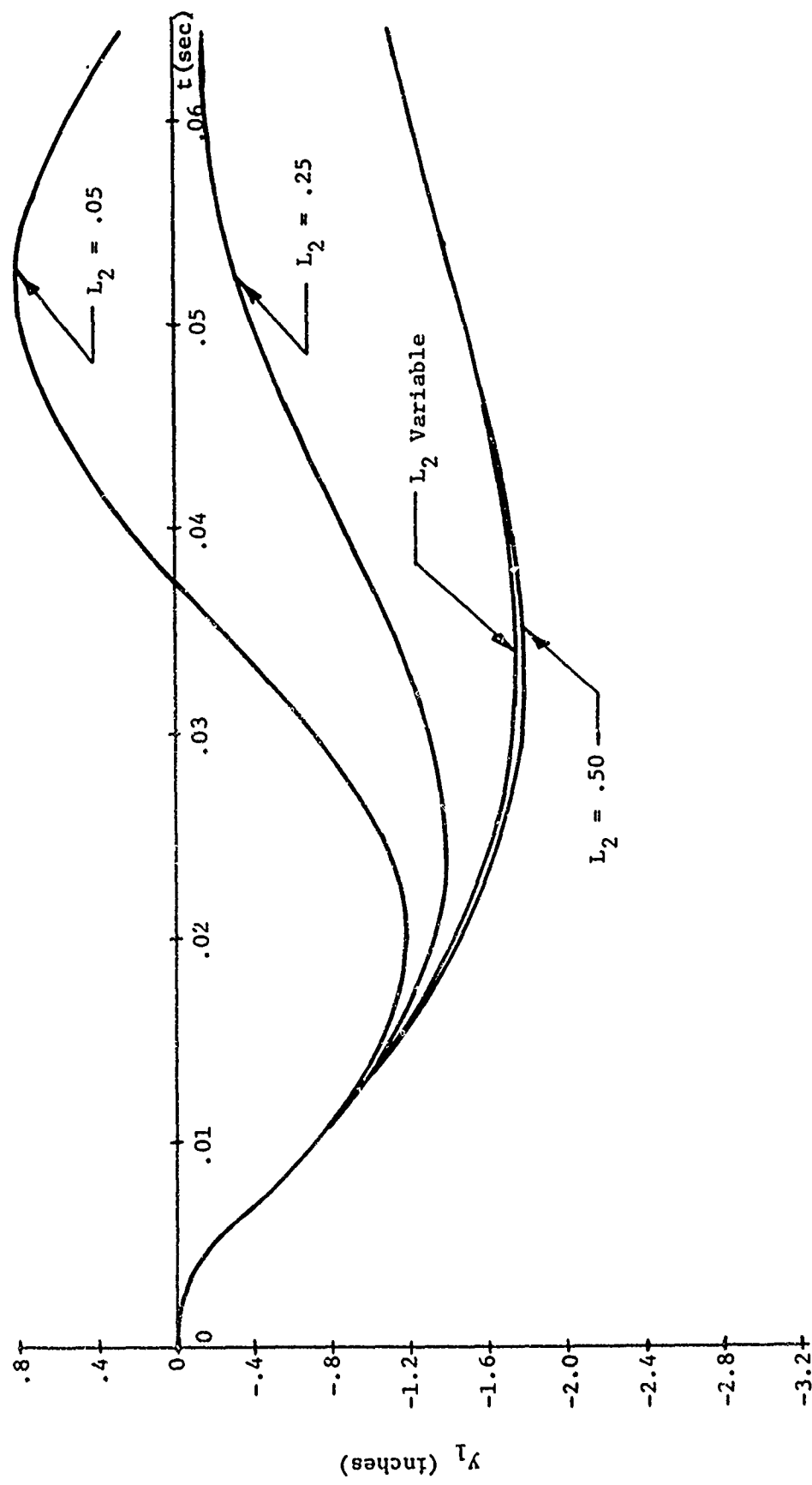


Fig. 21  $y_1$  vs.  $t$ ,  $R = .1$ ,  $L_2$  Variable Compared With  $L_2$  Constant

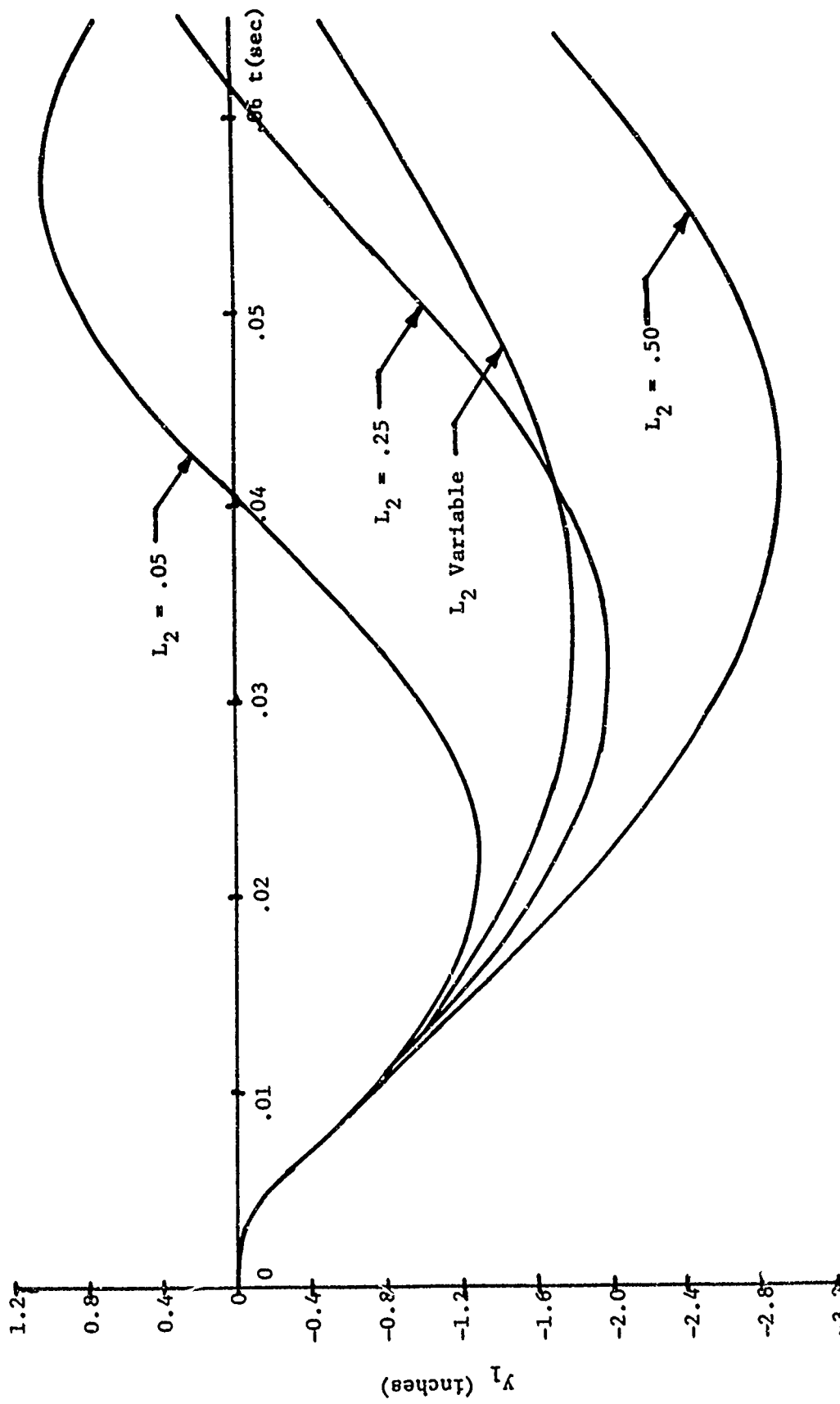


Fig. 22  $y_1$  vs.  $t$ ,  $R = 1$ ,  $L_2$  Variable Compared With  $L_2$  Constant

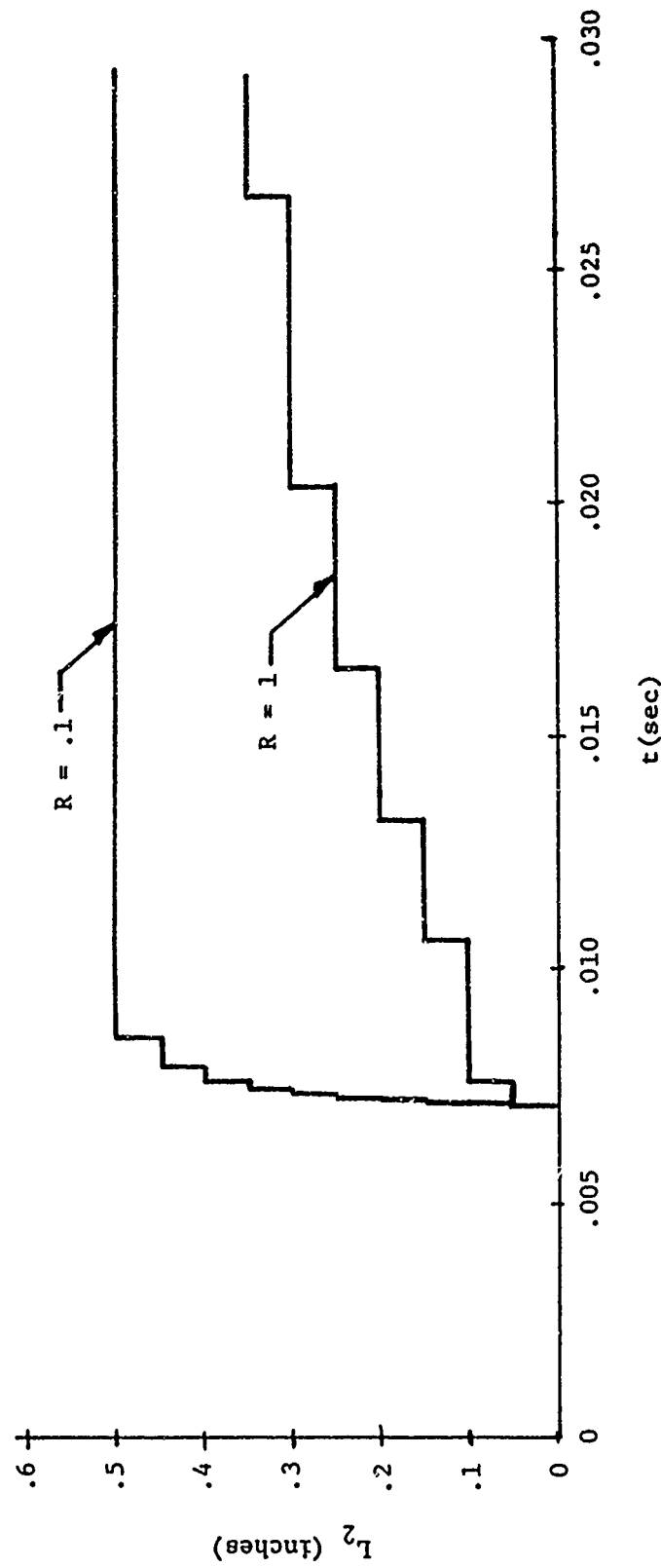


Fig. 23  $L_2$  vs.  $t$ ,  $R = .1$  and 1

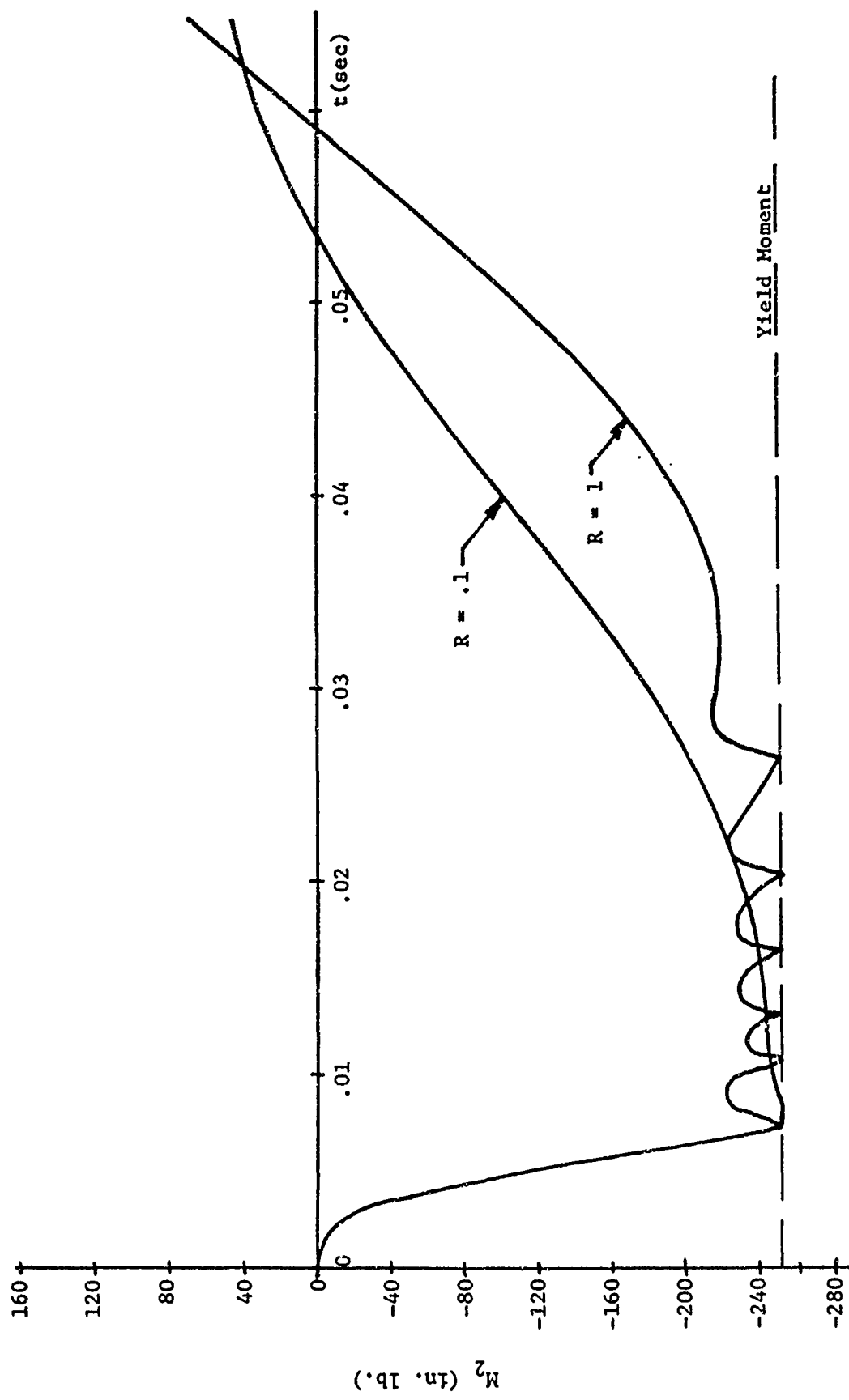


Fig. 24  $M_2$  vs.  $t$ ,  $L_2$  a Variable,  $R = .1$  and 1

## REFERENCES

1. Neubert, V. N., Rangaiah, V. P. and Vogel, W., "Shock Analysis of Structural Systems", Office of Naval Research Contract No. NONR-656(28) (X), Interim Report No. 9, February, 1970.
2. Stanovsky, J. J. and Neubert, V. H., "Shock Response of Beams with Non-Linear Material Properties", Office of Naval Research Contract No. NONR-656(28) (X), Interim Report No. 5, October, 1966.
3. Brown, W. G., "Dynamic Properties of Cold Rolled Steel", Masters Thesis, Department of Engineering Mechanics, The Pennsylvania State University, September, 1967.
4. Malvern, L. E., "The Propagation of Longitudinal Waves of Plastic Deformation in a Bar of Material Exhibiting a Strain Rate Effect", Trans. ASME, Journal of Appl. Mech., June, 1951.
5. Plass, H. J., "Theory of Plastic Sending Waves in a Bar of Strain Rate Material", Proc. 2nd Midwest Conf. on Solid Mechanics, Purdue University, pp. 109-134, 1955.
6. Vogel, W. H., "The Dynamic Response of a Viscoplastic Beam", Doctoral Thesis, The Department of Engineering Mechanics, The Pennsylvania State University, June, 1971.